ONLINE ADAPTATION OF USER STATE ESTIMATION IN A POWERED HIP EXOSKELETON USING MACHINE LEARNING

A Dissertation
Presented to
The Academic Faculty

By

Pratik Kunapuli

In Partial Fulfillment
of the Requirements for the Degree
Master of Science in the
School of Electrical and Computer Engineering

Georgia Institute of Technology

August 2020

ONLINE ADAPTATION OF USER STATE ESTIMATION IN A POWERED HIP EXOSKELETON USING MACHINE LEARNING

Approved by:

Dr. Aaron Young, Advisor
School of Mechanical Engineering, School of Electrical and Computer Engineering
Georgia Institute of Technology

Dr. Omer Inan
School of Electrical and Computer Engineering
Georgia Institute of Technology

Dr. Matthieu Bloch
School of Electrical and Computer Engineering
Georgia Institute of Technology

Date Approved: July 24, 2020

ACKNOWLEDGEMENTS

I would not have been able to present the work completed here without he following people. First and foremost, I would like to thank my advisor, Dr. Aaron Young, for his tremendous support, advice, and mentorship for this research. I would also like to express my gratitude to my friend and colleague, Inseung Kang, for without his guidance and partnership this research would not have been possible. I would also like to thank Jeff Hsu, Julian Park, and Henry Luk for their work in developing the powered hip exoskeleton device.

I would like to thank the undergraduate students for their support of the hip exoskeleton project and their assistance in conducting this research: Regu Nammalwar, Shahana Maji, Heejoo Jin, Alan Jin, Grace Choi, and Sung Kang. Without the time and effort given by these students, this research would have not been possible.

I would also like to thank the various members of the Exoskeleton and Prosthetic Intelligent Control Lab with whom I've had the privilege to work with: Dean Molinaro, Krishan Bhakta, Jonathan Camargo, and the rest of the graduate students. Along the many coffee runs, the emotional and mental support as well as the sharing of ideas has been greatly appreciated.

I would like to thank Dr. Omer Inan and Dr. Matthieu Bloch for serving as committee members for my thesis. Finally, I would like to thank my parents and brother. I love you and thank you for supporting me throughout my life.

TABLE OF CONTENTS

LIST OF TABLES

LIST OF FIGURES

SUMMARY

Powered exoskeletons are a wearable technology that seeks to use robotic power to augment the capabilities of the human using them. Lower limb exoskeletons in particular are designed to aid in mobility tasks, rehabilitation, and other forms of human ability augmentation. Hip exoskeletons apply assistance at the hip joint, one of the largest contributors to positive mechanical work during walking tasks and aim to reduce the energetic expenditure of the human by supplementing robotic power to this joint. Recent exoskeleton technology has grown immensely, and as hip exoskeletons are being developed, so are their control systems. These control systems rely on understanding information about the user and correspondingly applying robotic power in the form of an assistance profile to aid the user in walking. This user state estimation is a crucial part of exoskeleton control, as it directly affects the ability of users to walk and the efficacy of the exoskeleton.

In this thesis, a study of novel user state estimation techniques in various settings is presented. The first hypothesis investigated is that a machine learning-based gait phase estimation technique will reduce estimation error compared to time-based estimation techniques in treadmill walking with able-bodied subjects wearing the powered hip exoskeleton. The second hypothesis presented is that using biological sensor information with machine learning-based estimators for walking speed and inclination angle will reduce estimation error compared to machine learning-based estimators using only mechanical sensor data, specifically with elderly subjects with the powered hip exoskeleton. The final hypothesis presented is that online adaptation of deep learning-based models for gait phase and walking speed estimation will reduce estimation error compared to user-independent deep learning-based models for overground walking of able-bodied subjects wearing the powered hip exoskeleton.

Human subject testing is presented to test all of these hypotheses. The results from

the first experiment show that machine learning-based gait phase estimation outperforms time-based estimation in dynamic walking tasks such as acceleration or deceleration, and performs the same on steady-state walking. The results from the second experiment show that using biological sensor information reduces estimation error for walking speed and inclination angle compared to using only mechanical sensors for both able-bodied and elderly subjects. Finally, the preliminary results from the third experiment show that online adaptation of deep learning-based models reduces the estimation error for gait phase and walking speed estimation compared to user-independent models.

CHAPTER 1

INTRODUCTION

1.1 Background

Over the past decade, lower-limb exoskeleton technology has been a focus of both academic and industrial research. The potential applications of these exoskeletons in human augmentation, wearable robotics, and rehabilitation, have prompted numerous recent exoskeleton technology improvements [1, 2]. Because of the large contribution of positive mechanical work by the hip joint in ambulation tasks [3], the hip joint serves as a logical choice for exoskeletons to target. Numerous hip exoskeletons have been developed to study control strategies with the aim of reducing energetic expenditure of walking [4, 5, 6, 7]. As exoskeleton control strategies are being developed, a clear need for feedback information about the human wearing the device to the robotic exoskeleton has developed. As such, user state estimation has become an important factor for exoskeleton development.

One of the most critical aspects of user state estimation for hip exoskeletons is gait phase estimation. Since no part of the robotic apparatus comes in contact with the ground, on-board sensors must be used to detect various gait event timings such as heel contact [1]. Often, this gait phase is represented as a percentage, between 0% and 100% where 0% corresponds to a heel contact of a certain stride of a particular leg and 100% corresponds to the heel contact of the next stride for the same leg [8] (Fig. 1.1). Hip exoskeletons use this variable to define assistance profiles for their control strategies. As such, accurate estimation of gait phase is paramount for exoskeletons to provide assistance to the user at the proper timing during the ambulation tasks [7, 9].

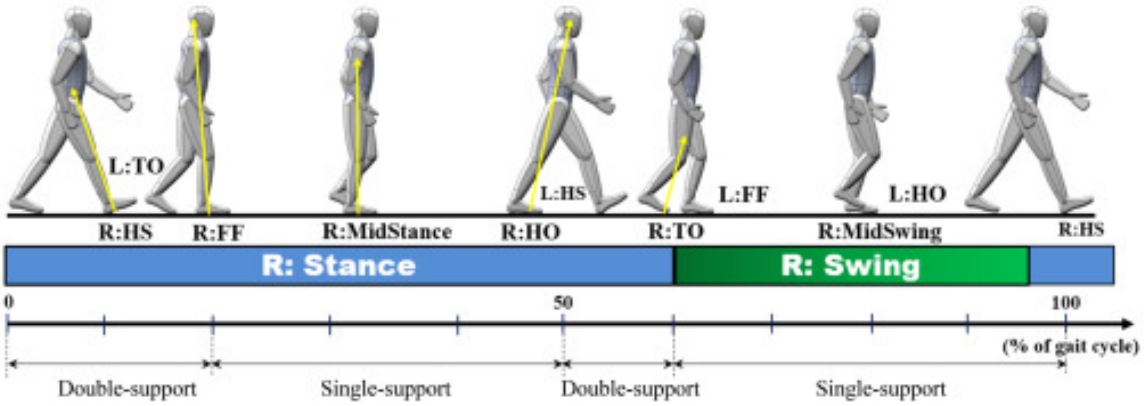

Figure 1.1: Illustration of gait cycle with corresponding gait phase percentage and biomechanical gait events. Source: [8]

1.1.1 User State Estimation Techniques

Various techniques have been used to estimate gait phase in hip exoskeletons. One such strategy is to use time-based estimation techniques coupled with a distally placed mechanical sensor such as a force sensitive resistor (FSR) placed on the heel [10, 11] . The mechanical sensor measures ground contact, and the time between these events can be recorded and averaged over a number of strides. This method works well for constant speed walking such as that of treadmill walking but, given the number of steps needed to average, this method fails to dynamically adapt to speed changes without a time delay in the estimation. Another method is to use a phase variable mapped from the hip angle, measured by a joint encoder [12, 13]. This method maps a roughly sinusoidal hip joint angle into a linearly increasing phase variable. While this method is more robust compared to the time-based estimation methods, it still requires rhythmic motion and fails to accurately estimate gait phase during dynamic motion. Finally, an adaptive oscillator is another method used for gait phase estimation, where the frequency envelope of the joint trajectory is modeled and then used to produce torque at a matching frequency [5, 14, 15]. This method performs better than the previous two methods but is much more complex, requires subject-specific tuning and still has some delay under dynamic motion since it relies on sinusoidal motion.

Another user-state variable that is relevant to hip exoskeletons is walking speed. This variable is important to scale assistance and match biomechanical performance of human walking [16]. Some methods to estimate this variable include integrating accelerations and gyroscope measurements from a distally mounter inertial measurement unit (IMU) [17, 18]. Another method is to use machine learning to learn the sequence of IMU signals in a recurrent neural network (RNN) [19]. While these methods have shown success in estimation performance, they rely on being placed distally, often outside of the region of a hip exoskeleton orthosis such as on the shank. In terms of environmental estimation, slope estimation contains useful feedback information for the device control law in a similar fashion to walking speed estimation. Common methods for slope estimation are to use a mechanical sensor such as an IMU [18], but the pitfalls of this method are the slow update rate and sensor drift over time, making this method undesirable for real-time applications.

1.1.2 Machine Learning

A possible solution to address the lack of high fidelity and real-time user state estimation is machine learning combined with sensor fusion techniques [20]. In the context of a hip exoskeleton, using sensor fusion allows the mechanical sensor data to be combined together in meaningful ways that can be exploited to provide user state estimation in real-time with higher accuracy. Additionally, the common pitfalls of using mechanical sensors such as IMUs would be mitigated since machine learning algorithms can learn the inherent drift in the sensor data. Finally, since on-board sensor data is used in these machine learning models, the learned representation is based on a configuration of the exoskeleton, meaning it is robust to dynamic movement of the user. Although there is a plethora of machine learning models being developed and researched, neural networks have gained recent attention for their use in deep learning tasks [21], and the power of neural networks to learn difficult tasks via a ”black box” approach is well documented [22]. One additional benefit

of using neural networks is their ease of implementation in real-time hardware due to the inherent simplicity of matrix multiplication.

Some research groups have implemented machine learning algorithms to learn user state variables on various robotic devices. In particular, gait phase estimation has been performed on robotic prosthesis devices [23], and using single sensor approaches from distally placed sensors with a hip exoskeleton [19]. However, these methods needed an additional sensor or were classifying the gait phase into discrete labels rather than estimating a continuous variable. To the author's knowledge, there has not been an investigation into using purely on-board sensors for a hip exoskeleton to develop continuous gait phase estimation in real-time. Further extending these principles, using machine learning to estimate walking speed and inclination angle has not been investigated from on-board sensors on a hip exoskeleton.

Machine learning paradigms often require an immense amount of data to learn a task well [21]. This tends to yield issues in human subject testing, which is required for machine learning applications for human augmentation robotics, since it is physically taxing for data to be collected. Thus, user-independent systems have been developed to leverage data across multiple different users rather than collecting an immense amount of data from a single user. Fundamentally this differs from a traditional machine learning paradigm [24] where the data used for training and testing would be from the same task (in this case, specific user). Comparisons between these user-independent models and the traditional form, user-dependent, have been made for intent recognition algorithms on prosthetic devices [25]. Furthermore, methods to adapt from a user-independent model to a user-dependent model have been explored in the context of using biological sensors for prosthetic devices which may degrade over time [26]. This online adaptation seeks to improve the machine learning-based estimator's accuracy by leveraging new user-specific data in real-time. This task has been implemented for classification tasks [27] and intent recognition [26], but to

the author's knowledge has not been used to improve machine learning-based estimators of continuous user state variables in real-time on a hip exoskeleton.

1.1.3 Hip Exoskeleton Device

The hip exoskeleton device used for the experiments in this thesis is an autonomous hip exoskeleton. This device is capable of providing 60 Nm of assistance, and features a closed loop series elastic actuator design for torque tracking [28]. This exoskeleton is controlled by a microprocessor coupled with an FPGA (myRIO, National Instruments, USA). The device hosts two absolute magnetic encoders (Orbis, Renishaw, UK) measuring hip angle at 100 Hz, one at each joint. Additionally, there are three IMUs (Micro USB, Yost Lab, USA), one on each thigh cuff and the last on the trunk, measuring linear accelerations in three axes and rotational velocities in three axes at 100 Hz each. Lastly, FSRs can be optionally attached on the heel of the device user in order to detect heel contact with the ground (Fig. 1.2).

1.2 Hypotheses

In this thesis, a study of machine learning-based user state estimation techniques is presented in various forms and with online adaptation. The first hypothesis presented is that a machine learning-based gait phase estimation technique will reduce estimation error compared to time-based estimation techniques in treadmill walking with able-bodied subjects wearing the powered hip exoskeleton. The second hypothesis presented is that using biological sensor information with machine learning-based estimators for walking speed and inclination angle will reduce estimation error compared to machine learning-based estimators using only mechanical sensor data, specifically with elderly subjects with the powered hip exoskeleton. The final hypothesis presented is that online adaptation of deep

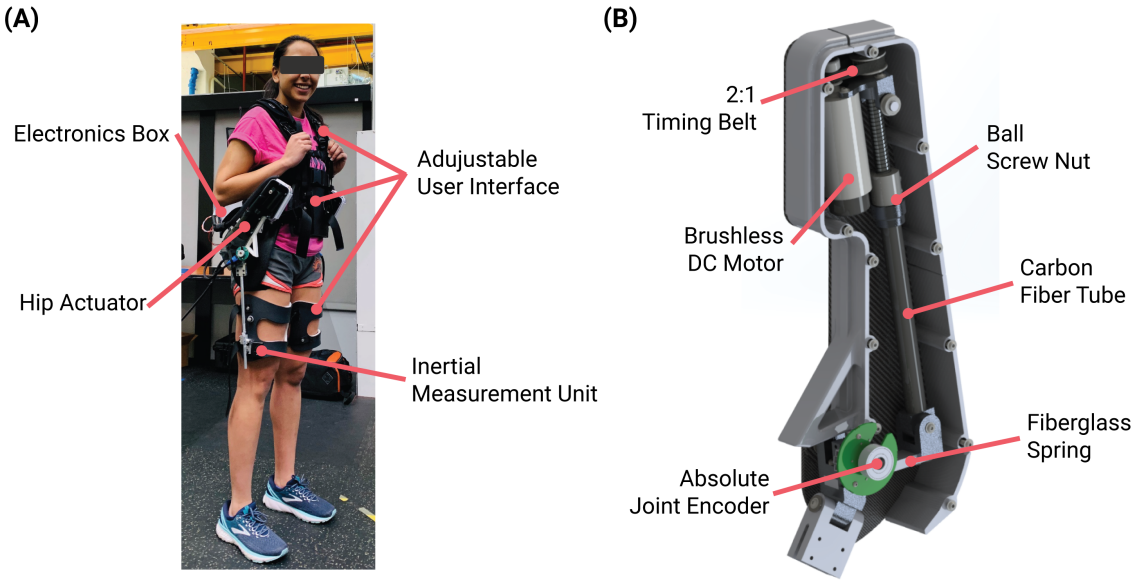

Figure 1.2: Hip exoskeleton device. (A) The exoskeleton features actuators attached bilaterally at the waist and the electronics box attached to the back. Various on-board sensors are labeled. (B) The actuator detailing the use of a carbon fiber spring in a closed loop series elastic actuator. Source: [29]

learning-based models for gait phase and walking speed estimation will reduce estimation error compared to user-independent deep learning-based models for community walking of able-bodied subjects wearing the powered hip exoskeleton. The rest of the thesis is organized as follows. Chapter 2 details the experiment, results, and discussion surrounding the first hypothesis: the use of machine-learning based gait phase estimation compared to time-based estimation. Chapter 3 details the experiment, results, and discussion surrounding the second hypothesis: the role of electromyography (EMG) in speed and slope estimation using machine learning. Chapter 4 details the development of deep learning-based estimators for gait phase and speed estimation using on-board mechanical sensors. Chapter 5 details the experiment, results, and discussion surrounding the final hypothesis: the effect of online adaptation on user state estimation for overground walking.

CHAPTER 2

NEURAL NETWORK-BASED GAIT PHASE ESTIMATION

A study was performed to develop a machine learning-based gait phase estimator and compare it to the state-of-the-art time-based estimation strategies for treadmill walking on a powered hip exoskeleton. The hypothesis presented was that the sensor fusion-based machine learning model can estimate a user's gait phase with lower error compared to an event detection method using a mechanical sensor during dynamic speed locomotion tasks. A sub-hypothesis was that a machine learning model trained to estimate gait phase from a specific user's data will yield less error than a machine learning model trained in a generalized user-independent fashion. To test these hypotheses, the powered hip exoskeleton was used to collect data in an initial experiment, various neural network-based gait phase estimators were developed, and the models were finally tested against a time-based estimation technique on a dynamic speed profile on a treadmill in a second validation experiment. The goal of this study was to evaluate the feasibility of implementing neural network-based estimators in real-time, as well as to understand the importance of subject specific data in machine learning models for human augmentation robotics.

2.1 Initial Data Collection

The study was approved by the Georgia Institute of Technology Institutional Review Board, and informed written consent was obtained for all subjects. Eight healthy subjects with an average age of 22.3 $\pm$ 2.4 years, height of 1.77 $\pm$ 0.06 m, and body mass of 74.4 $\pm$ 7.6 kg were asked to walk on the treadmill (TuffTread, USA) with the powered hip

exoskeleton for 2 minutes at walking speeds ranging from 0.6 m/s to 1.0 m/s with an increment of 0.05 m/s for a total of 18 minutes. The exoskeleton was put into zero impedance mode, meaning no active assistance was applied but the interaction torque between the subject and the device was minimized for transparency of motion, for all 9 conditions. During all walking conditions, mechanical sensor data from the right thigh and trunk IMUs, the hip joint angle from the encoder, and the heel contact information from the force sensitive resistor (FSR) sensor (for ground truth labeling) were recorded.

2.2 Offline Model Optimization

Raw FSR voltage was used to label the heel contact as an event marker. Each rising edge of the FSR voltage marked a heel contact, and between two consecutive heel contacts the gait phase was labeled as a linearly increasing signal from 0% to 100%. However, this results in discontinuities in the gait phase percentage, as the signal would go from 99% to 0% suddenly. This discontinuity presents an issue when using the gait phase label in loss functions for training neural networks, as the large discontinuity would be seen as a large error but temporally this error is much smaller. To avoid this discontinuity, the gait phase percentage was transformed into a phasor representation on the unit circle and the Cartesian coordinates were used as the ground truth label instead of the raw gait phase percentage (Fig. 2.1). Equations 2.1- 2.3 are used to transform the gait phase percentage, g, into the pair (x, y) which is used to train the models. The angle representation θ accounts for the discontinuity between 0% and 100%. The loss function was defined as the mean squared error between the estimate and the ground truth in the polar representation (Equation 2.4).

$$\theta = \frac{g}{2\pi \cdot 100} \tag{2.1}$$

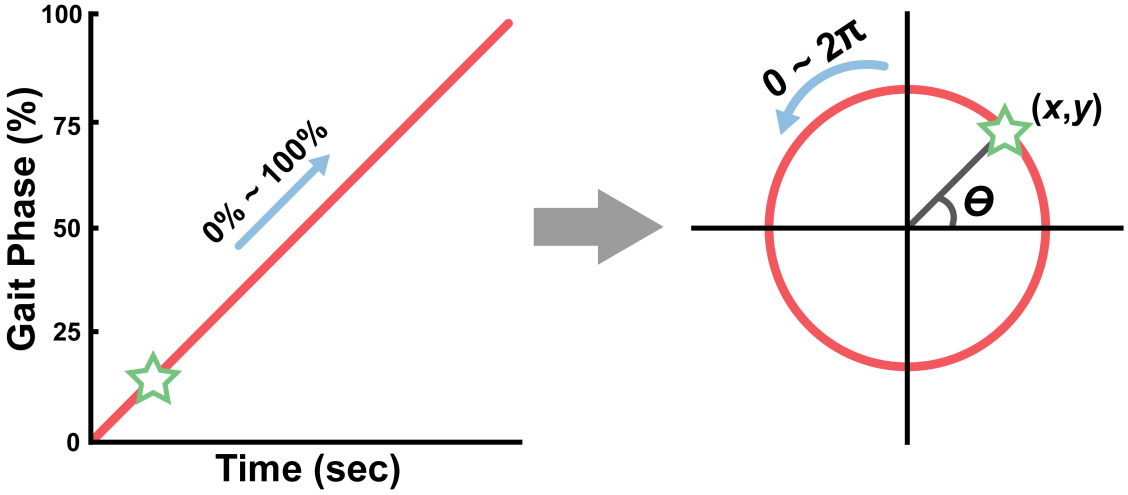

Figure 2.1: Gait phase output conversion. To eliminate the inherent discontinuity of a gait phase output (where 100% is equal to 0%), the signal is converted to a unit polar coordinate system where the gait phase is represented as Cartesian coordinates. An example of gait phase conversion is shown with a green star. Source: [30]

$$x = \cos(\theta) \tag{2.2}$$

$$y = \sin(\theta) \tag{2.3}$$

$$l = \frac{1}{N}\sum_{i=1}^{N}(Y_i - \hat{Y}_i)^2 \tag{2.4}$$

A baseline neural network of a single layer and 20 neurons was used to evaluate the feature-dependent hyperparameters such as the sliding window length and which features were relevant. Following previous methods of extracting features from mechanical sensor data on powered human augmentation devices [31], six features were computed for each mechanical sensor signal within a sliding window: min value, max value, mean value, standard deviation, first (least recent) value, and last (most recent) value. The sensor signals collected were the hip encoder angle, three Euler angles from the thigh IMU and three

Euler angles from the trunk IMU, and the six features were computed for all seven of these signals resulting in a total of 42 features. The length of the sliding window was an optimized parameter and of all the options tested, the length of 300 ms performed the best in the baseline neural network. After the sliding window length was locked down, sequential feature selection and sequential sensor selection was performed to rank the most relevant sensors and features. This is useful in machine learning tasks where the amount of data that can be collected is limited and thus to robustly learn the underlying task, the least relevant features can be removed from the dataset [32].

Sensor selection yielded machine learning model errors of 9.20 $\pm$ 1.92% with the hip encoder only, 5.65 $\pm$ 1.83% with the hip encoder and thigh IMU, 7.56 $\pm$ 2.77% with the hip encoder and trunk IMU, and 6.55 $\pm$ 1.62% with all sensors. This optimization sweep demonstrated that the hip encoder and the thigh IMU contained the most relevant information for estimating gait phase percentage (Fig. 2.2). The sequential forward feature selection confirmed the results from the sensor selection and additionally, showed that the Z-axis (transverse plane) Euler angles were much less favored compared to the X-axis (sagittal plane) or the Y-axis (frontal plane) Euler angles.

After finalizing the dataset with the features and ground truth, three different fully connected neural network models were created to optimize the estimation task from the data. The models differed in the amount of user-specific data they contained. The first model was the user-independent model (IND), where the model is trained on all subject except for one subject and then tested on the subject that was withheld. This model represents a generalized model applied to a new user, leveraging a large amount of data from a collection of other users [25]. A second model was the user-dependent model (DEP), where the model is trained on a subset of data from a single user and then tested on the remaining data from that same selected user. This model represents a user-specific model aimed at optimizing the accuracy as much as possible by solely learning a single user's gait patterns. Finally, a

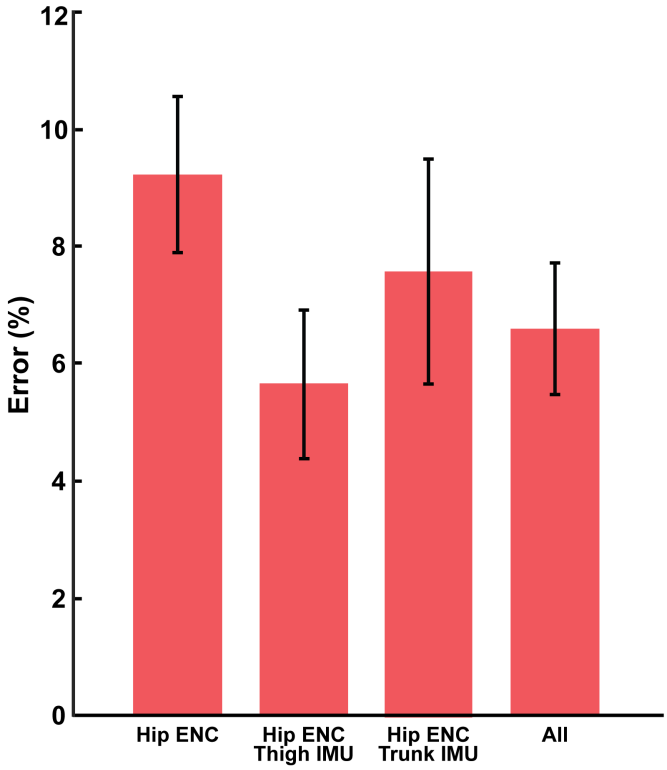

Figure 2.2: Sensor selection error results. Machine learning model error was measured with various sensor combinations to find the minimum number of sensors with lowest error. Error bars in the graph represent the 95% confidence interval. Source: [30]

combination of the two previously proposed models is presented: a semi-dependent model (SEMI), where the model starts from a pre-trained IND model and then additionally trains on a small subset (half) of a single user's data with higher weighting and is tested on the rest of that single user's data. Following a transfer learning approach, this SEMI aims to maximize the accuracy for a single tested user while minimizing the data needed from that user since it can leverage data from other users. All of the neural networks were trained in Python using Keras [33] with a TensorFlow [34] backend.

In order to maximize estimation accuracy, standard methods were used to sweep neural network parameters and were evaluated on a common dataset from all subjects (IND) [35]. When evaluating any set of neural network parameters, a leave-one-subject-out cross validation strategy was used to generalize performance across any unseen user to be tested on. The size of the first layer is fixed from the number of features selected via the optimization performed earlier (17), and the output of the network is fixed by the labeling paradigm (2). Sweeping through numerous layers yielded minimal improvements in accuracy for more than one hidden layer. With the real-time implementation in mind, a single hidden layer was chosen, since it minimizes the computation complexity while maximizing the model's accuracy. Following a similar process, the number of neurons, optimizer, learning rate, activation function, and batch size were selected by sweeping through different values and selecting the combination with the highest accuracy. The final hyper-parameters selected were 20 neurons in the hidden layer, a Stochastic Gradient Descent (SGD) optimizer with Nesterov acceleration [36, 37], a learning rate of 0.001, $\tanh$ activation function, and a batch size of 128. For the SEMI model there is one unique parameter that does not exist for the other models, the relative importance of the specific user data compared to the other subjects, and it was swept through resulting in a weighing of 80:1 which maximized accuracy. All models were trained for a maximum of 200 epochs with early stopping criteria monitoring the validation loss, stopping if the computed loss of the withheld validation set was minimized to prevent from overfitting. After the neural network parameters were

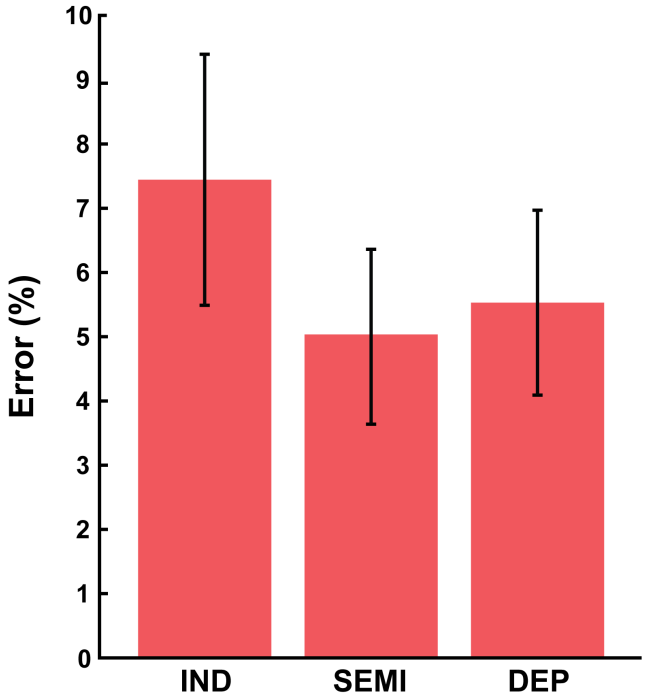

Figure 2.3: Offline comparison of gait phase estimator error across different user models. Error bars in the graph represent the 95% confidence interval. Source: [30]

optimized, the feature optimization was performed again on the optimized neural network model rather than the baseline neural network model to ensure the features chosen were still the best, and the results were the same. With optimal neural network hyper-parameters, resulting models had errors of 7.44 $\pm$ 2.82%, 5.04 $\pm$ 1.96%, and 5.53 $\pm$ 2.08% for the IND, SEMI, and DEP models respectively. (Fig. 2.3).

2.3 Methods

2.3.1 Experimental Protocol

The study was approved by the Georgia Institute of Technology Institutional Review Board, and informed written consent was obtained for all subjects. For experimental validation of the gait phase estimator, ten healthy subjects different from the original eight

healthy subjects from the initial data collection with an average age of 21.3 $\pm$ 1.8 years, height of 1.79 $\pm$ 0.06 m, and body mass of 75.1 $\pm$ 4.9 kg were initially asked to walk on a treadmill for 5 minutes with a powered hip exoskeleton and treadmill speed ranging from 0.6 m/s to 1.0 m/s using a predefined speed profile (Fig. 2.4A). This initial walking trial was used as to collect training data for the models which required user-specific data (DEP and SEMI). During this training trial, the hip exoskeleton was controlled in a zero impedance mode, and the relevant sensor data from the pilot experiment (the hip encoder and thigh IMU) were collected, as well as the FSR sensor for ground truth labeling only. After the DEP and SEMI models were generated on a seperate computer, subjects walked for 3 minutes on the treadmill with a powered hip exoskeleton for each condition where the first minute had a constant walking speed of 0.8 m/s, the second minute had a predefined speed profile ranging from 0.6 m/s to 1.0 m/s, and the third minute had a predefined speed profile ranging from 0.8 m/s to 1.1 m/s (Fig. 2.4B). The maximum walking speed was defined based on the capabilities of the exoskeleton, as this was the highest walking speed at which the device could track torque accurately.

The testing speed profile was chosen to represent and validate estimator performance in three walking tasks: constant walking speed, dynamic walking within the speed range of the training data, and in dynamic walking outside the speed range of the training data (to observe model's capability in extrapolation). During walking, four different gait phase estimator methods were implemented: time-based estimation (TBE) using FSR sensor, and three machine learning-based estimators presented earlier (IND, DEP, and SEMI). For all walking conditions, the tested gait phase estimator generated a sinusoidal torque command with a peak torque magnitude set to 1 Nm. Because the testing speed profile examines three aspects of the estimator performance, the results were segmented into three parts. Part A corresponds to the first section in the trial representing the steady state walking speed. Part B corresponds to the second section representing the dynamic movement where the walking speed is changing in the same range that the machine learning models were trained. Lastly,

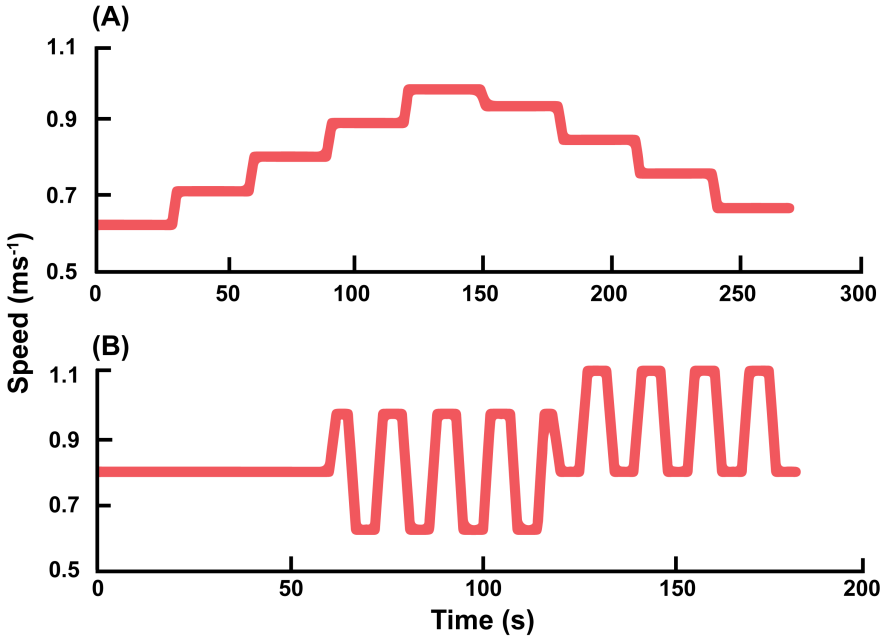

Figure 2.4: Treadmill speed profile for experimental validation of the gait phase estimator. (A) Speed profile for the training trial. The data collected was used to generate the user-dependent and semi-dependent models. (B) Speed profile for testing the gait phase estimators. The profile was set to evaluate model accuracy in a dynamic speed range settings. Source: [30]

Part C corresponds to the dynamic movement where the walking speed is changing in a range not entirely within the range that the machine learning models were trained.

2.3.2 Real-Time Implementation

Implementing the neural network-based models in the control architecture was simple due to the nature of neural networks to be reproduced via matrix multiplication. The overall matrix computation of each neural network model can be represented by Equations (2.5) and (2.6), where F is the feature vector of size 17×1, H is the hidden layer vector of size 20×1, and G is the output vector of size 2×1. W_i represents the weight matrix at layer i, and B_i represents the bias vector at layer i. Depending on which model is selected to be used for the real-time testing, the matrices W_1, W_2, B_1, and B_2 will be loaded from memory as text files. In order to convert from the model output back to gait phase percentage, which is used by the exoskeleton controller, Equation (2.7) is used. g represents the gait phase percentage, and x and y represent the individual outputs of the model.

$$H = W_1 \cdot F + B_1 \tag{2.5}$$

$$G \triangleq \begin{bmatrix} x \\ y \end{bmatrix} = W_2 \cdot \tanh(H) + B_2 \tag{2.6}$$

$$g = (\tan^{-1}(\frac{y}{x}) + 2\pi) \mod 2\pi) \cdot \frac{100}{2\pi} \tag{2.7}$$

2.3.3 Torque Generation

Using the real-time gait phase estimation, torque is applied to the left and right actuators according to Equations (2.8) and (2.9) respectively. A sinusoidal torque is commanded to both sides of the device. The peak torque of 1 Nm (extension) appears at 0% gait cycle and 1 Nm (flexion) at 50% of the gait cycle for each leg to represent the hip extension and flexion assistance.

$$\tau_{right} = \cos(g \cdot \frac{2\pi}{100}) \tag{2.8}$$

$$\tau_{left} = -\cos(g \cdot \frac{2\pi}{100}) \tag{2.9}$$

2.3.4 Statistical Analysis

The FSR sensor was used to calculate the ground truth gait phase percentage, and the corresponding ground truth torque profile was generated by applying Equations 2.8 and 2.9. All results were computed by comparing the gait phase estimation and torque applied to the ground truths and calculating the root mean squared error (RMSE). A repeated measures one-way ANOVA test was conducted to compare the estimator performance across the three parts, and a Bonferroni post-hoc correction (α = 0.05) for a pairwise comparison across multiple measures was applied.

2.4 Results

Overall, the machine learning methods performed well in real-time and outperformed the time-based estimation method in dynamic speed conditions. An example of real-time

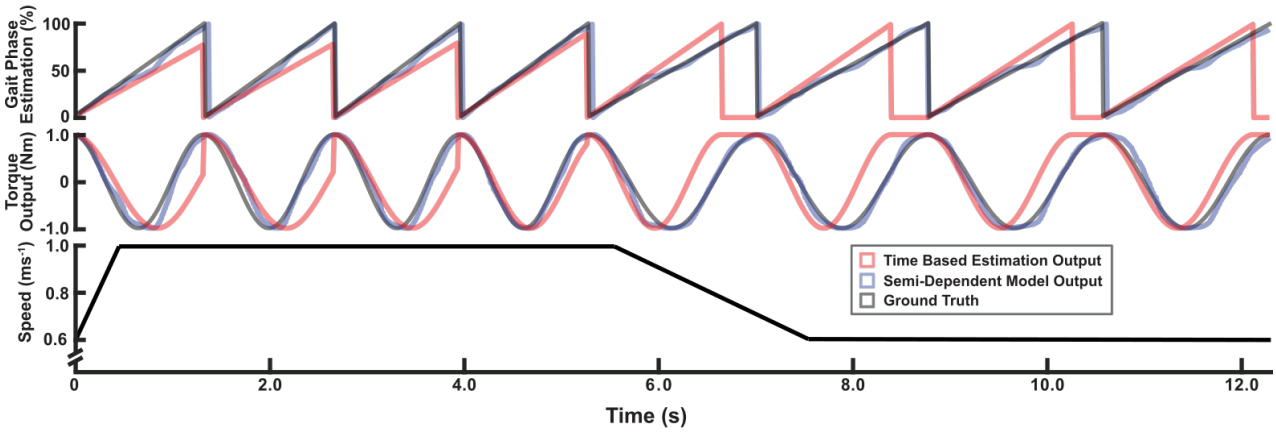

Figure 2.5: Real-time performance of both the time-based estimation (TBE) and the SEMI model against the ground truth over 8 steps with the corresponding walking speed. When the walking speed either accelerates (0s - 0.5s) or decelerates (5.5s - 7.5s), the TBE takes several additional steps to update the gait phase estimation while the SEMI is capable to adapting to dynamics speed change instantaneously. Due to poor estimation during dynamic speed ranges, the resultant torque profile generated from the TBE has discontinuities while the SEMI does not. Source: [30]

estimation of gait phase using machine learning-based technique compared to the time-based estimation technique and the resultant commanded torque is shown over eight steps from the powered hip exoskeleton (Fig. 2.5). Real-time gait phase estimation results are shown in Figure 2.6, where the results are segmented based on the type of motion as well as presented as an average across the ten subjects with 95% confidence interval per estimator used.

2.4.1 Real-Time Gait Phase Estimator Performance

In the steady state portion (Fig. 2.6A), none of the strategies performed significantly differently for gait phase estimation or the resulting torque generation. However, in the dynamic conditions (Fig. 2.6B and C), both the SEMI and DEP machine learning strategies significantly ($p < 0.05$) outperformed the TBE method. Additionally, in the dynamic condition with higher speed range (Fig. 2.6C), the SEMI model performed significantly better than the IND model ($p < 0.05$). These statistical trends were consistent between

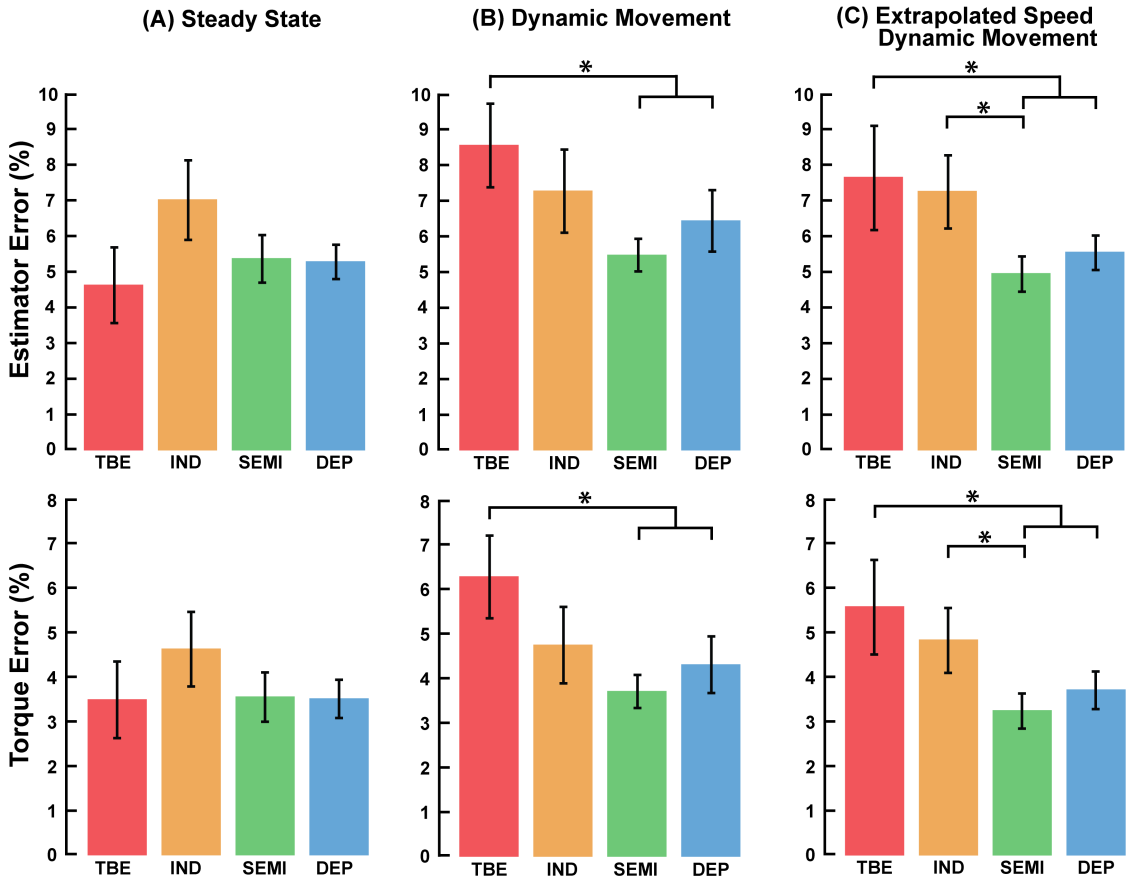

Figure 2.6: Real-time gait phase estimation results. The speed trial had three parts to comprehend dynamic speed changes to evaluate the estimator performance. (A) Overall performances were similar during steady state walking speed where the TBE performed the best. (B) During the dynamic speed changes within the speed range of training dataset, the SEMI performed the best. (C) Similar trends to (B) were shown for the dynamic speed changes with speed range outside of the training dataset where all user models were able to extrapolate and estimate the gait phase correctly and the SEMI performed the best. Asterisks indicate the estimator that had significantly lower error between two conditions in the pairwise Bonferroni post-hoc test. Data were averaged across ten subjects and the error bars in the graph represent the 95% confidence interval. Source: [30]

both the RMSE of the gait phase estimator and the torque generation.

In summary for torque generation during dynamic movements (Fig. 2.6B and C), the IND reduced average torque generation error by 18.9% ($p = 0.55$), SEMI by 40.9% ($p < 0.05$), and DEP by 32.4% ($p < 0.05$) compared to the TBE strategy. A further investigation was performed on these trials to quantify the estimation accuracy by differentiating the dynamic trials into steady-state speed and dynamic speed sections. The average RMSE for the steady state section were 4.83 $\pm$ 0.62% and 5.07 $\pm$ 0.49% while the dynamic section average RMSE were 26.75 $\pm$ 9.13% and 7.18 $\pm$ 1.56% for the TBE and SEMI, respectively across all subjects.

2.4.2 Training Time of SEMI and DEP Models

The SEMI and the DEP were both trained on the user-specific data from the training trials. The SEMI converged for a much lower number of epochs, representing the number of times observing the training set compared to the DEP. On average across subjects, the SEMI converged after 43.80 $\pm$ 5.28 epochs. The DEP converged on average after 174.60 $\pm$ 12.71 epochs.

2.5 Discussion

The primary contribution of this study was to develop and evaluate a sensor fusion-based machine learning model for estimating user gait phase in real-time using a powered hip exoskeleton. Overall, all three of our proposed gait phase estimators performed either similar or better than the baseline TBE across all three walking conditions. Specifically, during the dynamic trials, the machine learning models outperformed the TBE (as shown in Fig. 2.5) where the TBE either leads or lags in the estimation when the user is changing

speeds as indicated by the increased RMSE compared to the steady-state section. These results clearly illustrate the power of machine learning having superiority over the TBE when the user is dynamically accelerating or decelerating. This corresponds to our original hypothesis that the neural network-based model can adapt to different walking speeds because of the prior gait phase pattern that the model has seen from the training dataset. The significance of our models handling the dynamic tasks is that these tasks resembles closely to what people would experience in the real-world where speed is dynamically changing and starting or stopping motions are common.

The key difference within the machine learning models was the amount of user-specific data trained on by each model. The IND is the most convenient model out of the three models as it requires no new data from the user. This means that for any new user, no additional data needs to be collected for a robust machine learning-based gait phase estimator to be used in real-time. However, the IND does not perform better than the TBE during the steady state speed and only slightly better during the dynamic tasks. On the other hand, the SEMI and DEP are trained on and able to learn the user- specific gait pattern to significantly outperform the TBE during the dynamic tasks including the extrapolated speed ranges. Naturally, this comes with the cost of collecting the user-specific data in the first place. Overall, the SEMI performed the best among the machine learning models because it aims to maximize the accuracy for a given subject while utilizing the general dataset which contains different gait pattern variations across other subjects. The difference in performance between the SEMI and DEP models shows that the transfer learning-based approach using a pre-trained model learns gait dynamics better than simply learning from the tested user alone. Furthermore, the SEMI trains for a much smaller number of epochs than the DEP, which represents the fact that less user- specific data is needed to learn by leveraging the IND to train from. However, there may be limitations to any model, such as when collecting a large pool of data is not feasible (due to patient pool limitations), or collecting user-specific data is expensive (due to population capabilities).

In our experiment, a mid-level controller (sinusoidal wave) was chosen so that gait phase estimation errors from the TBE would be mitigated, especially at the heel contact (0 or 100%), in order to ensure a smooth torque output to the user. This was due to the fact that in dynamic motion, TBE would either estimate heel contacts early or late, and by biasing the controller to output similar torques around the heel contact whether the gait phase was before or after heel contact. Because of this, the TBE had a slight advantage compared to other estimators when comparing the torque error, since errors around heel contact were mitigated by the sinusoidal nature of the torque controller chosen. This would not be the case if the torque generation was not symmetric about the heel contact (0% gait phase), and errors would be expected to be higher.

The machine learning models presented outperformed different methods that have been used in previous studies. The baseline method TBE, adopted by several groups for their exoskeletons due to its simplicity, did not yield robust estimation results during the dynamic tasks as predicted [11, 38]. Moreover, even during steady state walking, the TBE method did not show any significant benefits (approximately 2.5% error difference compared to the worst performing of the machine learning models, IND). Considering its performance, the results indicate that the TBE is appropriate for experiments with a fixed treadmill speed but is not appropriate for dynamic tasks. Other groups have implemented more advanced methods for estimating gait phase such as phase variables or adaptive oscillators which can be more adaptable and continuously estimate the gait phase [39, 40, 41]. Specifically, using a hip angle to map a phasor has substantially more gait phase estimation error than the sensor fusion approach [12, 13]. By using only hip angles and estimating gait phase with a neural network, the model has 63% more error than when combining it with IMU information. One large hurdle for the adaptive oscillator approach is the detailed subject tuning and a higher computational burden when considering real-time implementation on a microprocessor. Additionally, while this oscillator method performs in similar orders of magnitude compared to the machine learning approach during steady state or gradual

speed changes, it cannot robustly accommodate abrupt changes in the user walking speeds (specifically when accelerating) [14], which is very possible in real-world settings, limiting the feasibility of this approach for overground walking.

One limitation of this study is that the device training and testing profile was conducted in controlled speed ranges on a treadmill. While this was mainly done to systematically compare the estimator performance equally, this does not fully capture real-world over ground locomotion that would likely have even higher variability and dynamics than the simulated tasks for this study. The results from this study show an exciting promise for the future direction of exoskeleton control. The SEMI model showcased the power of transfer learning [42] applied to the human-augmentation robotics domain, where the user-specific data is both highly valued and costly to attain. For example, in a clinical setting, it might not be feasible to collect so much data from the patient due to their limited mobility. In this case, the SEMI model using less additional user data compared to the DEP model may be a viable solution. By having accurate user gait phase information, the exoskeleton controller can be tuned to more smoothly provide assistance to the user compared to simpler state machines. Both the SEMI and DEP strategies minimized error across all conditions and could potentially be viable options for gait phase estimation for exoskeleton devices in a variety of tasks including overground walking.

CHAPTER 3

ELECTROMYOGRAPHY (EMG) CONTRIBUTIONS IN SPEED AND SLOPE ESTIMATION

Exoskeleton devices are designed to operate in all modes of ambulation and thus will encounter a variety of environmental and user conditions. Two of these conditions that directly affect the ability of the exoskeletons to be used overground is walking speed and inclination angle. A study was performed to develop speed and slope estimation techniques following previous work using machine learning-based estimators, as well as to evaluate the benefit of using biological signals in addition to mechanical sensors such as electromyography (EMG). The hypothesis presented is that using biological sensor information with machine learning-based estimators for walking speed and inclination angle will reduce estimation error compared to machine learning-based estimators using only mechanical sensor data on the powered hip exoskeleton for both able-bodied subjects and elderly subjects. To test this hypothesis, subjects walked using the powered hip exoskeleton to collect data, various neural network-based speed and slope estimators were developed, and the resulting models were evaluated on their performance offline for both subject pools. The goal of this study was to evaluate the contribution of EMG sensor data to the tasks of speed and slope estimation, specifically using neural networks and for various populations with different gait dynamics.

3.1 Methods

3.1.1 Experimental Protocol

The study was approved by the Georgia Institute of Technology Institutional Review Board, and informed written consent was obtained for all subjects. Four able-bodied subjects (three males and one female) with an average age of 23.5 $\pm$ 3.3 years, height of 1.79 $\pm$ 0.08 m, and body mass of 73.3 $\pm$ 4.6 kg and two elderly subjects (both females) with an average age of 72.5 years, height of 1.67 m, and body mass of 73.5 kg participated in data collection. Both of the elderly subject were capable of community ambulation but walked with a reduced preferred walking speed by approximately 60%. All subjects wore the powered hip exoskeleton as they were asked to walk on the treadmill (Bertec Corperation) (Fig. 3.1A). During all conditions, the exoskeleton controller was set to zero impedance mode, mitigating any interaction torque between the user and the device. During walking, data was collected from the hip joint encoder, an IMU placed on the trunk, an IMU placed on the thigh cuff, and eight electromyography (EMG) channels were collected using surface EMG (Biometrics Ltd). Of the eight EMG channels, six were placed within the thigh cuff region on each subject, and two were placed outside this region on proximal hip musculature (Table 3.1). This was done so that the EMG could be segmented into two different classifications: a pattern-based EMG placement, and a targeted muscle-based placement.

The experiment was conducted in two parts: static and dynamic trials. During static trials, the able-bodied subjects walked on a level ground with speed ranging from 0.8 m/s to 1.2 m/s in 0.1 m/s increments for one minute each, totaling five minutes. Next, the subjects walked at incline with slope ranging from 2° to 10° in 2° increments and decline with slope ranging from -2° to -10° in 2° increments at walking speeds of 0.8 m/s for one minute each, totaling 10 minutes. For elderly subjects, the same protocol was followed except treadmill speeds and slope angles were set within their capabilities of ambulation.

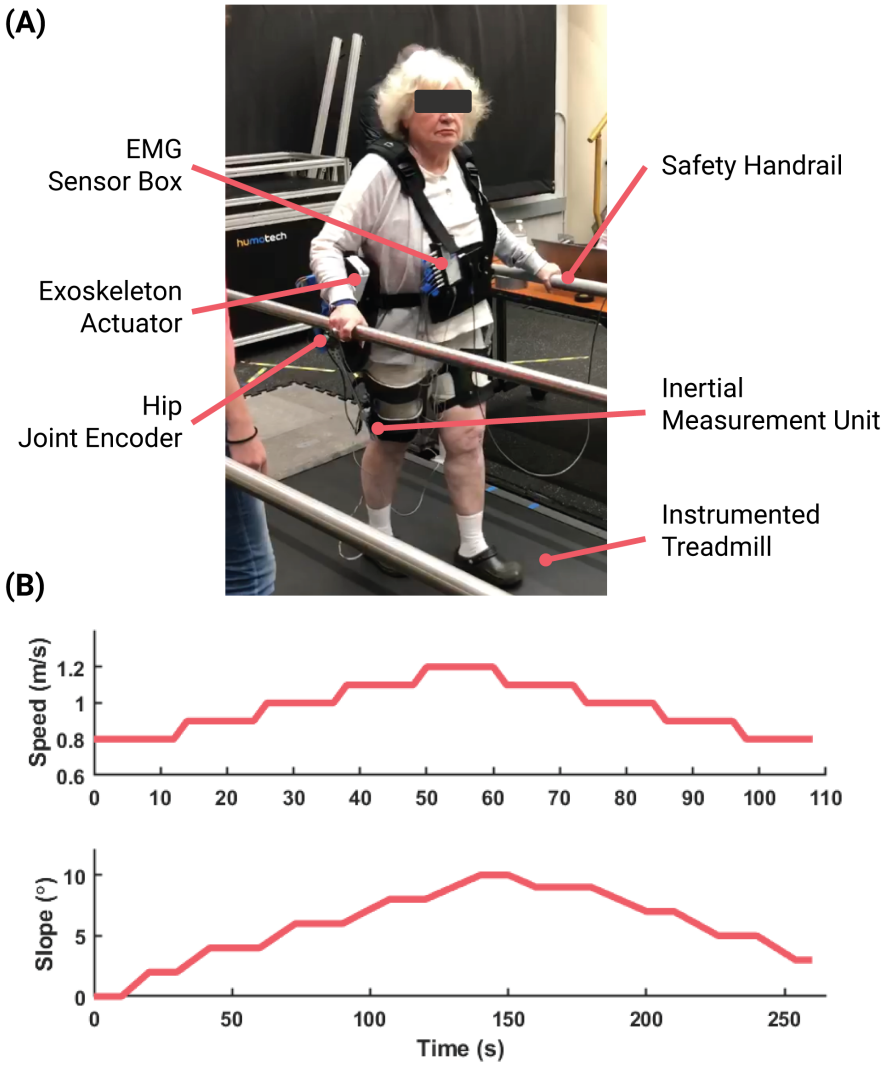

Figure 3.1: Experimental setup for data collection. (A) The subject walked on the treadmill at a variety of speeds and slopes. During each trial, hip joint encoder angle, data from the thigh IMU, data from the trunk IMU, and eight channels of electromyography (EMG) data was collected. (B) The speed profile showcased a dynamic trial for able-bodied subjects where the walking speed dynamically changed as the user walked. Similarly, a profile was developed for inclination angle. Source: [29]

Table 3.1: EMG channels collected during experimentation. Channels 3-8 were placed within the exoskeleton thigh cuff region, where as channels 1 and 2 were placed on the proximal hip musculature. Adapted from: [29]

Channel Number	Muscle Targeted	Abbreviation
1	proximal rectus femoris	PRF
2	gluteus medius	GM
3	rectus femoris	RF
4	biceps femoris	BF
5	vastus medialis	VM
6	vastus lateralis	VL
7	adductor magnus	AM
8	distal biceps femoris	DBF

The treadmill speed range was set from 0.3 m/s to 0.7 m/s with 0.1 m/s increments and slope range was set from 1° to 7° with 2° increments with walking speed of 0.3 m/s.

During dynamic trials, the able-bodied subjects walked on a treadmill while the speed and slope (both incline and decline) were modulated by a predefined trajectory generated from the control desk (MATLAB, MathWorks). The speed profile contained both steady state section ranging from 0.8 m/s to 1.2 m/s as well as dynamic section where the treadmill modulated speed by accelerating and decelerating for 2 minutes (Fig. 3.1B). Similar profiles were generated for both incline and decline dynamic trials where the slope angles ranged from 2° to 10° both uphill and downhill walking at 0.8 m/s for 3 minutes. Similar to the static trial, elder subjects followed the same protocol except for slower walking speeds and slope angles to their ambulation capabilities. For elder subjects, dynamic speed profile ranged from 0.3 m/s to 0.7 m/s for 2 minutes and slope profile ranged from 1° to 7° both uphill and downhill walking at 0.3 m/s for 3 minutes.

3.1.2 Machine Learning Model Development

After the data collection, all EMG data was processed with a bandpass filter (8th order Butterworth, 20 Hz - 400 Hz) to remove any motion artifacts. For each subject, three different neural network models were generated from speed and slope walking conditions using different underlying sets of sensors. The first set of data contained only the mechanical sensors on the hip exoskeleton: hip encoder angle, 6-axis IMU on the thigh, and 6-axis IMU on the trunk. The second dataset combined the mechanical sensor data with 6 of the EMG channels representing the pattern-based placement approach (channels 1-6) (EMG1). The last dataset combined the mechanical sensor data with a different subset of 6 EMG channels representing the targeted muscle-based placement approach (channels 3-8) (EMG2). To ensure the model comparison was fair between the two EMG datasets, the number of channels was kept the same. For slope estimation, separate models were developed for incline walking and decline walking. Although using a single, unified model for both incline and decline estimation is possible, separating the tasks significantly reduced the error, and since locomotion mode classification can be done robustly [43, 44], this is a feasible approach for real-time slope estimation.

Speed and slope estimation was performed once per gait cycle to maximize performance of the model. Due to the fundamental nature of the much slower rate of change of the label compared to the sensors, estimating once per gait cycle had lower error compared to estimating continuously as gait phase estimation is done. The point chosen in the gait cycle was the peak hip extension angle, as this was a reliable gait event marker to detect from the on-board sensors. A sweep was performed of the length of the window for the feature extraction process. The sweep went from 50ms to 750ms in 50ms increments. The window length that maximized performance was at 500ms. With this window length, for mechanical sensors 4 features were extracted: minimum value, maximum value, mean value, and standard deviation. For the datasets with EMG channels, a single feature was

used: mean absolute value. The neural network architecture and hyperparameters were swept using common practices [35]. The finalized model had a single hidden layer with 50 nodes, activated by the $tanh$ function and was optimized by stochastic gradient descent. Although a larger number of nodes and layers may have yielded higher performance, this set was chosen for its feasibility of implementation in real-time on the hip exoskeleton which has fixed computation ability. Using this fixed neural network architecture, the three previously described datasets were used to train the models and they were evaluated using the root mean squared error (RMSE) loss function. During testing of the static trials, 5-fold cross validation was performed to prevent over-fitting while a single trial was withheld as the testing set and folded upon to generate the overall error. During the testing of the dynamic trials, the full static trial set was used to train via 5-fold cross validation and the entire dynamic trial was used as the testing set.

3.2 Results

3.2.1 Static Trial Performance

For able-bodied subjects (Fig. 3.2A), the average walking speed RMSE across all static trial conditions were 0.094 $\pm$ 0.043 m/s, 0.077 $\pm$ 0.012 m/s, and 0.076 $\pm$ 0.017 m/s for MECH, EMG1, and EMG2, respectively. For inclined slope estimation, the average RMSE were 1.624 $\pm$ 0.400° 1.288 $\pm$ 0.176° and 1.431 $\pm$ 0.307° for MECH, EMG1, and EMG2, respectively. For declined slope estimation, the average RMSE were 1.620 $\pm$ 0.633° 1.533 $\pm$ 0.608° and 1.324 $\pm$ 0.494° for MECH, EMG1, and EMG2, respectively. For elderly subjects (Fig. 3.2B), the average walking speed RMSE across all conditions were 0.061 m/s, 0.078 m/s, and 0.089 m/s for MECH, EMG1, and EMG2, respectively. For incline estimation with elderly subjects, the average RMSE was 1.363°, 1.556° and 1.604° for MECH, EMG1, and EMG2, respectively. For the decline, the average RMS errors were

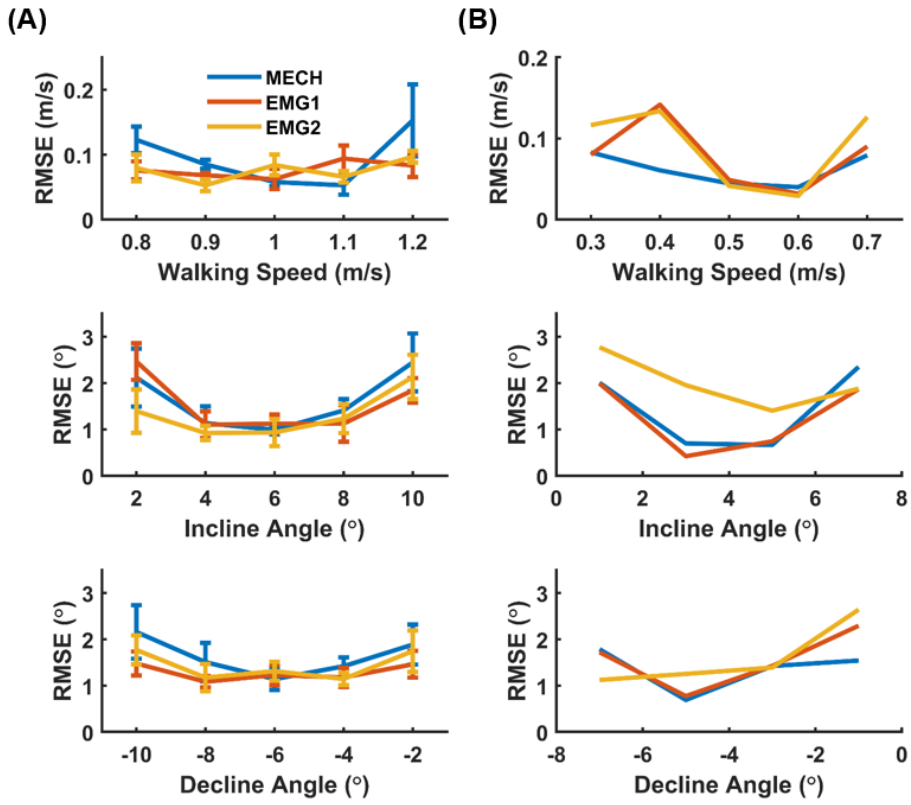

Figure 3.2: Static trial model performance for walking spede, inclination angle, and declination angle estimation. Colored lines represent models trained with different datasets. Root mean squared error (RMSE) was averaged across all users and error bars represent ± 1 standard error of mean (SEM). (A) Able-bodied subjects. (B) Elderly subjects. [29]

1.431°, 1.258°, and 2.003° for MECH, EMG1, and EMG2, respectively.

3.2.2 Dynamic Trial Performance

For able-bodied subjects (Fig. 3.3A) during dynamic trials, EMG1 and EMG2 reduced the average walking speed RMSE compared to the MECH dataset by 15.2% and 23.3%, respectively. For the incline estimation in dynamic trials, EMG1 and EMG2 reduced the average RMSE compared to the MECH dataset by 7.6% and 11.5%, respectively. For the decline slope estimation in dynamic trials, EMG1 and EMG2 reduced the RMSE compared to the MECH dataset by 14% and 4.8%, respectively. For elderly subjects (Fig. 3.3B) during dynamic trials, EMG1 reduced the average walking speed RMSE compared to the

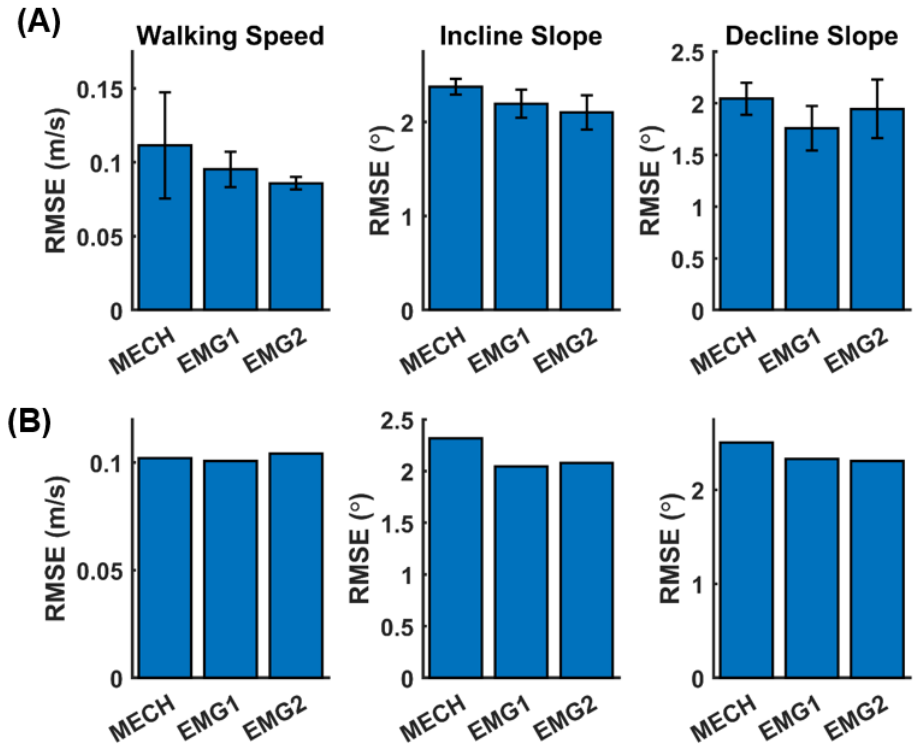

Figure 3.3: Dynamic trial performance for (A) able-bodied subjects and (B) elderly subjects. Root mean squared error (RMSE) was averaged across all users and error bars represent $\pm$ 1 standard error of mean (SEM). [29]

MECH dataset by 1%. For the incline estimation in dynamic trials with elderly subjects, EMG1 and EMG2 reduced the average RMSE compared to the MECH dataset by 11.8% and 10.2%, respectively. For the decline estimation in dynamic trials with elderly subjects, EMG1 and EMG2 reduced the average RMSE compared to the MECH dataset by 7% and 7.9%, respectively.

3.3 Discussion

Overall, neural networks were able to estimate walking speed and inclination angle with acceptable levels of accuracy regardless of the dataset used to train the models. For able-bodied subjects, models trained with EMG data had better performance than the models trained only with MECH data by reducing the average estimation error rate by 13.5% and

14.8% across all trials for EMG1 and EMG2, respectively. While the able-bodied results indicate consistent performance of both EMG models in all cases, the results were not the same for the elderly subjects. For elderly subjects, models trained with EMG outperformed the MECH model with an average error rate reduction of 6.6% and 5.4% for EMG1 and EMG2, respectively. This decrease in the relative benefit of adding EMG data can be attributed to many factors: limited sample size, slower range of speeds and inclines tested, as well as varying gait dynamics between populations. Although EMG contains useful information about user intent, it also is highly variable as a signal and thus may not be as good as an indicator for environmental or user state variables such as walking speed or inclination angle in the case where walking dynamics are varying such as with elderly subjects. Overall, the machine learning models benefited from the addition of EMG data indicating the potential benefit of using biological sensors for user state estimation.

One of the main reasons the EMG models were able to outperform the MECH models in the dynamic trials is due to the change of state compared to the static trials. In the static trials, the label of speed or incline is constant throughout the trial, and since data is collected continuously, numerous windows of data are seen for the same output label and the models are tasked with fitting a regression from these datapoints. However, in the case of dynamic trials, there are certain steps that occur during acceleration or deceleration for walking speed or when inclination or declination angle is changing. These instances are where EMG data is able to accurately predict the dynamic change of the output variable due to it's role in intent recognition [25, 45]. In more realistic settings such as overground walking, where starting or stopping motion is possible, EMG information may be valued even higher than it was in the cases tested by this study, and could potentially reduce estimation error significantly compared to using mechanical sensors only. One limitation of using EMG data is the subject specific nature of the signal, as well as the high variation between testing instances and numerous other characteristics such as placement, skin conductivity, etc. that could highly affect the ability of machine learning-based models to predict user state.

One main finding of this study was the way in which walking speed and slope estimation interacts with gait phase. Because of the slower rate of change of the state variables compared to sensors, models which estimated less frequently performed better. Estimating at a single time throughout the gait cycle for walking speed and inclination estimation performed the best compared to multiple times. Estimating continuously throughout the gait cycle using a unified model is an option, but estimating once per gait cycle out performed this method during offline optimization of the models. Although EMG information is valuable for estimating speed and inclination angle with higher fidelity compared to mechanical sensors only, it is not enough to continuously estimate these variables in real-time with high accuracy.

CHAPTER 4

DEEP LEARNING FOR GAIT PHASE AND WALKING SPEED ESTIMATION

As exoskeleton technology progresses, an understanding of how to optimally assists users in different conditions needs to be investigated. For this, overground walking presents a challenging task as two user state variables need to be estimated in tandem: gait phase and walking speed. The importance of accurate user state estimation has been demonstrated, and efforts to develop low error estimators for walking speed and gait phase estimation using neural networks has shown promising results [29, 30]. One key limitation of the previous methods used is the process of feature extraction being hand-picked. In the previous methods, a sliding window length was chosen and within the sliding window, signals were passed through a finite number of numerical functions such as mean, or standard deviation. However, deep learning methods suggest better forms of feature extraction can be learned rather than hand picked by the machine learning algorithm designer [24]. A study was performed to develop deep learning-based machine learning estimators for gait phase and speed estimation using mechanical sensor data from the powered hip exoskeleton. Additionally, given the user-specific gait dynamics seen in hip exoskeleton data even from able-bodied subjects, an investigation of learning from user-independent models on new data was performed. The hypothesis presented was that deep learning-based neural network models will outperform standard hand-picked models in gait phase and walking speed estimation from data on the powered hip exoskeleton. A sub-hypothesis presented is that learning from new data while estimating will reduce error compared to a user-independent model in simulation. To test these hypotheses, the powered hip exoskeleton was used to collect data from an initial pool of subjects, the data was then used to train neural network

models with various deep learning methods, and finally a simulation of adaptation was conducted offline. The goal of this study was to develop high accuracy machine learning-based user state estimation models with state-of-the-art machine learning techniques that could be re-implemented by other exoskeleton research groups to obtain reliable, low error user state estimation.

4.1 Initial Data Collection

4.1.1 Experimental Protocol

The study was approved by the Georgia Institute of Technology Institutional Review Board, and informed written consent was obtained for all subjects. The study was approved by the Georgia Institute of Technology Institutional Review Board, and informed written consent was obtained for all subjects. Eleven healthy subjects with an average age of 23.1 $\pm$ 1.7 years, height of 1.80 $\pm$ 0.05 m and body mass of 72.5 $\pm$ 4.98 kg were asked to walk on the treadmill (Bertec, USA) with the powered hip exoskeleton at walking speeds ranging from 0.3 m/s to 1.2 m/s at 0.1 m/s increments for one minute each, totaling 10 minutes of walking. Additionally, one subject walked for 10 minutes while the speed of the treadmill dynamically changed between 0.3 m/s and 1.2 m/s randomly, with steady-state speed sections of 30 seconds, and accelerations at 0.2 m/s/s 4.1. Mechanical sensor data was recorded such as the hip encoder angle, the right thigh IMU acceleration and gyroscope measurements, the trunk IMU acceleration and gyroscope measurements, as well as FSR voltages and treadmill speed for ground-truth labeling at 100 Hz.

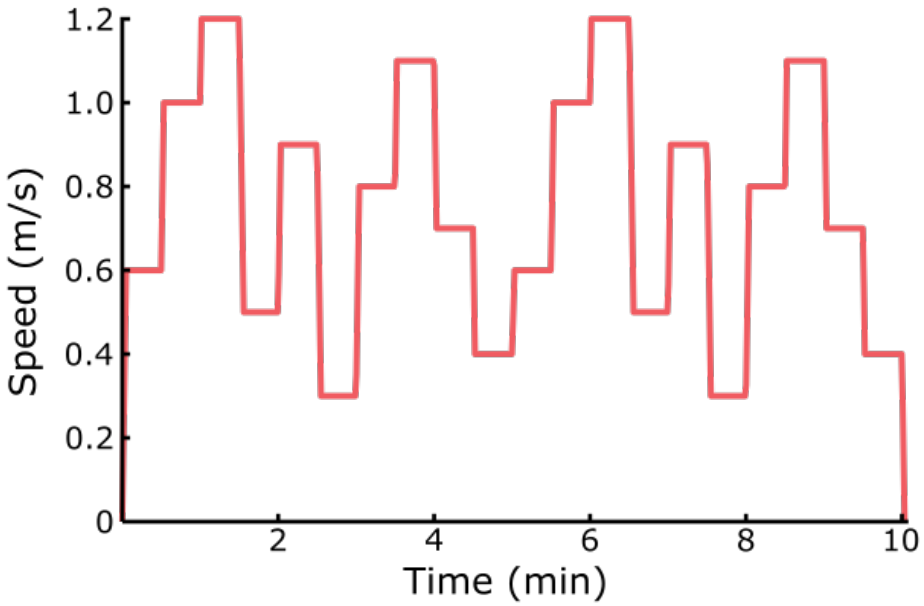

Figure 4.1: Speed profile used for the dynamic trial condition. Treadmill speed is modulated randomly with speeds between 0.3 m/s and 1.2 m/s with steady-state sections of 30 seconds. During dynamic speed changes, acceleration was set to 0.2 m/s/s.

4.1.2 Assistance Profile

During each trial, the powered hip exoskeleton was used and assistance was applied in the form of Equation 4.1, where g represents gait phase percentage for a single leg, s represents the walking speed, and $\mathcal{N}(\mu, \sigma^2)$ represents the Gaussian probability density function with mean μ and variance σ^2. The particular assistance profile chosen applies extension torque for the extension and flexion motions of the hip joint according to a Gaussian profile [5], rather than a trapezoidal assistance profile used in the past [7]. Additionally, the amount of total flexion assistance differs from the total amount of extension assistance. These were done to match hip joint kinetics more closely at different speeds.

$$\tau(g, s) = 10s\mathcal{N}(g - 5, 64) - 7s\mathcal{N}(g - 55, 64) + 10s\mathcal{N}(g - 105, 64) \tag{4.1}$$

4.2 Methods

4.2.1 Model Development

The dataset contained 13 sensor values and 2 labels, one corresponding to the gait phase percentage and the other to the walking speed. From this dataset, various machine learning models were developed for both gait phase estimation and walking speed estimation. For all gait phase estimation models, the gait phase percentage was transformed into the polar representation and the label was derived from the Cartesian coordinates because of the discontinuity in the gait phase label at heel contact [30]. Three different neural network models were developed for each gait phase and walking speed estimation: a fully connected neural network (FCNN) emulating the models previously used [30], a convolutional neural network (CNN) [46], and a Long Short Term Memory network (LSTM) [47]. The FCNN architecture was chosen because of its emerging use in the human augmentation robotics field. CNN architectures excel at tasks such as object recognition from camera imagery and although they are not as widely used in robotics, some applications have seen success integrating them into the control architecture [48]. LSTM architectures operate in a similar manner to CNN, but the recurrent nature of the architecture has enabled them to be successful in various user state tasks including walking speed estimation using a single sensor [19]. A sliding window approach was taken for all models, but they were implemented differently for the FCNN architecture compared to the CNN and LSTM architectures. For the the FCNN architecture, within the sliding window each sensor signal was converted to 6 features: min value, max value, mean value, standard deviation, first (least recent) value, and last (most recent) value. For the LSTM and CNN models, they operate on windows of data rather than discrete temporal instances, and the deep learning-based feature extraction meant that the raw sensor values were passed through the models. After initial layers of CNN or LSTM, dense layers could be added as the features would be learned in the in-

termediate representation. All models were trained as user-independent models: selecting a single testing user and removing them from the data set and training on the remaining 10 subjects. Additionally, all training was done with leave-one-subject-out validation and results were averaged across all 11 testing users.

4.2.2 Gait Phase Estimation

For gait phase estimation, each model was optimized independently to produce the best gait phase estimation technique per architecture. The window length was swept from 100ms to 1000ms in 50ms increments, and per architecture the best performing sliding window size was chosen. After the window length was finalized, there were individual hyperparameters associated with each model architecture that needed to be swept through. For the FCNN the hyperparameters to optimize were: number of neurons per layer, number of layers, activation function and the optimizer. For the CNN the hyperparameters to optimize were: convolution kernel shape, number of fully connected layers, activation function and the optimizer. For the LSTM the hyperparameters to optimize were: number of LSTM nodes, number of fully connected layers, activation function and the optimizer. Additionally, sequential forward feature selection was performed on the optimized model for FCNN just as previous methods, in order to reduce the dimensionality associated with the learning paradigm.

4.2.3 Speed Estimation

For speed estimation, each model was optimized independently to produce the best speed estimation technique per architecture. Like with the gait phase estimation models, the sliding window length was swept from 100ms to 1000ms for each model. For each model architecture, the same hyperparameters were swept through from the optimization

process developing the gait phase estimation models. One additional optimization process was performed for the speed models: how many models were to be used and when during the gait cycle they should estimate the walking speed. Ideally, a continuous model could be used but previous studies have shown how the error for continuously estimating throughout the gait cycle is much higher compared to at a single point in the gait cycle [29]. In order to further develop this idea, the number of models throughout the gait cycle was swept from 1 to 4, and for each number of model of contribution to the gait cycle was swept through.

Given the slow rate of change of the label compared to the sensor values, and the ideal task of continuous estimation throughout the gait cycle, the speed estimation models were very noisy in the output. To combat this for future real-time implementations, a Kalman filter was paired with the model output to reduce the noise in the estimation output. The dynamics of the Kalman filter were assumed to be constant, emulating constant walking speed and the measurement noise was taken as an average over a real-time buffer of outputs from the machine learning models. The variables that were tuned were the buffer length, the process noise and the initial measurement noise.

4.2.4 Simulation of Adaptation

A single subject walked during a dynamic trial where the walking speed was dynamically changing according to Fig. 4.1. This was done so the finalized gait phase and walking speed models could be tested on a simulation of overground walking where the speed can change randomly. Additionally, this data served as a test set for tuning of various real-time related parameters such as the Kalman filter variables for walking speed estimation. Finally, this data was used to simulate adapting to the new data while estimating in a real-time simulation, emulating transfer learning approaches. The simulation of adaptation had a number of parameters associated with it including rate of adaptation, learning rate for the gait phase estimation model, learning rate for the speed estimation model, weighting

of new data for the gait phase estimation model, and weighting of new data for the speed estimation models. A single user-independent model was tested which did not include the same user that walked for the dynamic trial in the training data.

4.3 Results

4.3.1 Gait Phase Estimation

For the FCNN model, the window length that achieved the highest performance was 400 ms. For CNN the optimized window length was 500 ms, and for LSTM the optimized window length was 350 ms. The best performing FCNN model had 3 hidden layers, in a 20-25-10-2 architecture. Each intermediate layer was activated by the $tanh$ function, and the final layer was activated by an identity function. The optimizer that performed the best was the AMSGrad optimizer [36] with a learning rate of 0.05. The best performing CNN model had 2 1-D convolutional layers and a single dense layer. The first convolutional layer captured a window length of 500ms and the kernel shape was 100ms over all 13 sensor values. The second convolutional layer captured a single kernel over the resulting 5x13 shaped input to produce a 1x13 feature vector. This feature vector was activated by the ReLU function, then a fully connected layer activated by tanh was used to estimate the gait phase in polar coordinates. The optimizer used for the CNN model was Adam [36], with a learning rate of 0.1. The best performing LSTM model had a single LSTM layer with 30 nodes, which was fed the 350 ms x 13 sensor signals. After the LSTM layer, a single dense layer was used and activated by $tanh$ to output the gait phase in polar coordinates. The optimizer used for the LSTM model was RMSprop with a learning rate of 0.01. The architecture for the best performing model is shown in Fig. 4.2.

The results comparing the best performing model for each architecture in gait phase estimation is shown in Fig. 4.3. All models were able to adequately learn to estimate gait

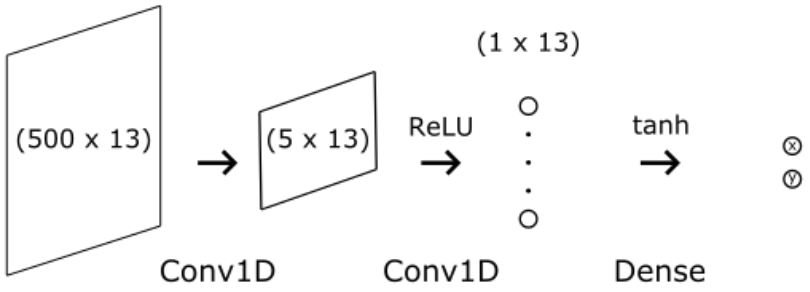

Figure 4.2: Model architecture for the best performing model in gait phase estimation. The Convolutional Neural Network (CNN) architecture performed the best and is comprised of a series of Conv1D and Dense layers.

phase, with the CNN and LSTM models performing better compared to the FCNN model. The best performing model was the CNN architecture, with an average RMSE of 4.74 $\pm$ 0.34%. The LSTM model had an average RMSE of 6.59 $\pm$ 0.22%. The FCNN model had an average RMSE of 8.40 $\pm$ 0.49%. Both the CNN model performance was significantly lower compared to the LSTM and FCNN ($p < 0.05$), and the LSTM model performance was significantly lower than the FCNN performance ($p < 0.05$).

4.3.2 Speed Estimation

Two different paradigms emerged for walking speed estimation: a single unified model estimating continuously throughout the gait cycle and a phase-dependent model, where 2 separate models were used: the first learning and estimating continuously from 0-60% of the gait cycle and the second learning and estimating continuously from 60-100% of the gait cycle. Both unified models and phase-dependent models were able to estimate walking speed, but the phase-dependent models performed better across all architectures.

For the FCNN model, the window length that achieved the highest performance was 500 ms. For CNN the optimized window length was 650 ms, and for LSTM the optimized window length was 650 ms. The best performing FCNN model had 2 hidden layers, in a 15-40-1 architecture. Each intermediate layer was activated by the sigmoid function, and the

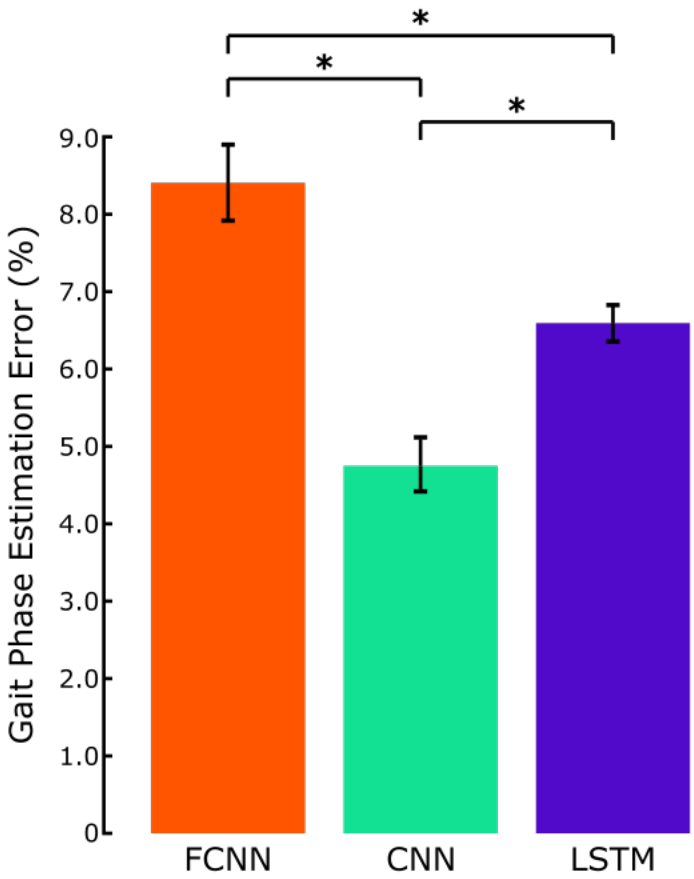

Figure 4.3: Gait phase estimation results per model architecture. The models were trained as user-independent models and the results were averaged across all 11 subjects being seen as novel testing users. Asterisk indicates a significant difference in error according to a pairwise Bonferroni post-hoc test. Error bars shown represent the standard error of mean (SEM).

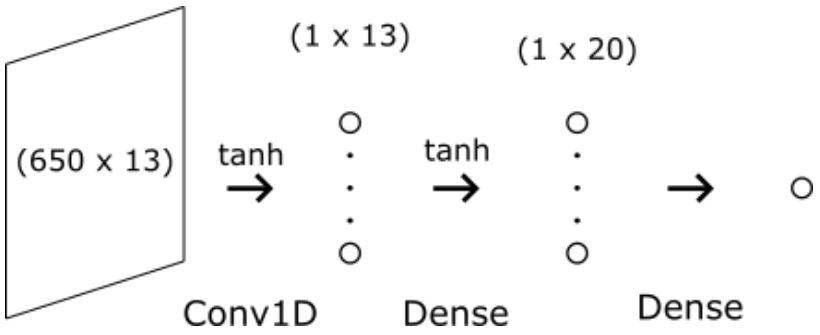

Figure 4.4: Model architecture for the best performing model in speed estimation. The Convolutional Neural Network (CNN) architecture performed the best and is comprised of a series of Conv1D and Dense layers.

final layer was activated by the identity function. the optimizer that performed the best was SGD with Nesterov momentum [36, 37], and a learning rate of 0.1. The best performing CNN model had a single 1-D convolutional layer with a kernel size of 650 ms across all 13 sensor signals, convolving down to a single 1x13 feature vector. From there, the feature vector was passed through 2 dense layers with a 13-20-1 node layout, each activated by $tanh$, and the final layer being activated by the identity function. The optimizer chosen was Adam with a learning rate of 0.05. For the LSTM model, the best perfoming architecture was a single LSTM layer with 20 nodes, which was fed the 650ms x 13 sensor singals, then passed through 2 dense layers in a 13-10-1 layout, with the hidden layer activated by $tanh$ and the final output activated by the identity function. The optimizer used was RMSprop with a learning rate of 0.01. The Kalman filter parameters were kept constant across models in order to evaluate them fairly. The optimized buffer length was 5 samples, the initial measurement noise was set to $1 * 10^{-7}$, and the process noise was set to $4 * 10^{-8}$. The architecture for the best performing model is shown in Fig. 4.4.

The results comparing the best performing model for each architecture in speed estimation is shown in Fig. 4.5. The best performing model was the CNN phase-dependent model, which had an average RMSE of 0.090 $\pm$ 0.008 m/s. The phase-dependent FCNN model had an average RMSE of 0.149 $\pm$ 0.007 m/s. The phase-dependent LSTM model

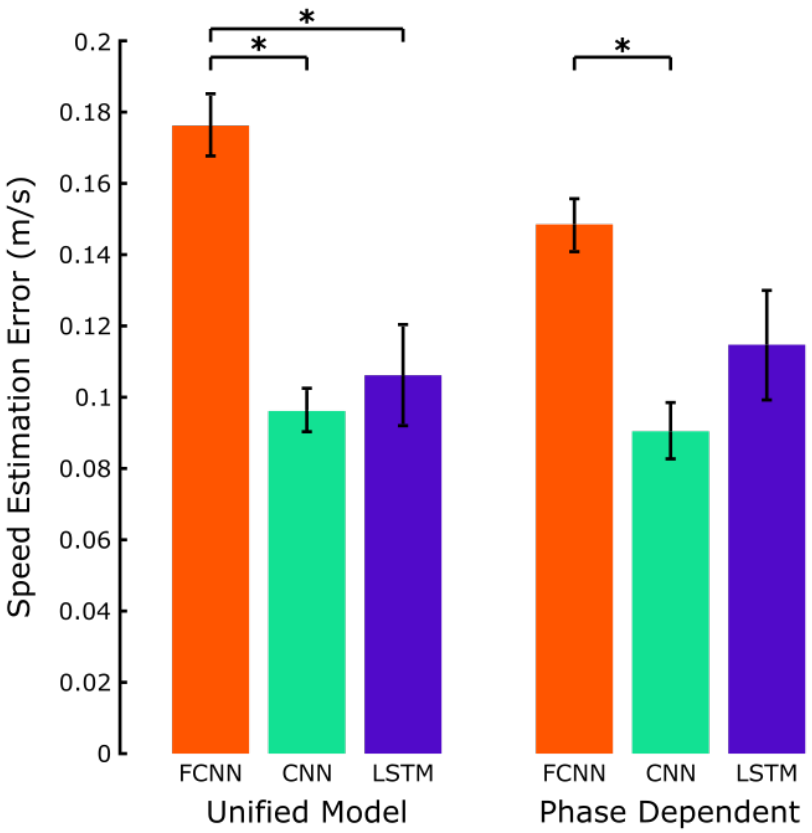

Figure 4.5: Speed estimation results per model architecture. Results are presented for both a single unified model estimating continuously throughout the gait cycle and a phase-dependent approach with multiple models estimating continuously throughout the gait cycle. The models were trained as user-independent models and the results were averaged across all 11 subjects being seen as novel testing users. Asterisk indicates a significant difference in error according to a pairwise Bonferroni post-hoc test. Error bars shown represent the standard error of mean (SEM).

had an average RMSE of 0.115 $\pm$ 0.015 m/s. The phase-dependent CNN model performed significantly better compared to the phase-dependent FCNN model ($p < 0.05$). The unified FCNN model had an average RMSE of 0.176 $\pm$ 0.008 m/s. The unified CNN model had an average RMSE of 0.096 $\pm$ 0.006 m/s. The unified LSTM model had an average RMSE of 0.176 $\pm$ 0.008 m/s. Both the unified CNN and unified LSTM model performed significantly better compared to the unified FCNN model.

4.3.3 Simulation of Adaptation

The simulation of adaptation from a user-independent model to new data while estimating performed well. Both gait phase estimation error and walking speed estimation error decreased, demonstrating the power of transfer learning techniques for user state estimation. For gait phase estimation, the adapted model performed significantly better than the user-independent model by the final minute of the trial ($p < 0.01$), reducing the gait phase estimation error by 68.98%. For speed estimation, the adapted model without the Kalman filter performed significantly better than the user-independent model without the Kalman filter ($p < 0.01$), reducing error by 33.71% by the final minute. The adapted model with the Kalman filter performed significantly better than the user-independent model with the Kalman filter ($p < 0.01$), reducing error by 50.98% by the final minute. The addition of the Kalman filter was successful in reducing the speed estimation error. The Kalman filter reduced the error significantly ($p < 0.01$) by 32.96% for the user-independent model by the final minute, and significantly ($p < 0.01$) reduced the error by 50.43% for the adapted model by the final minute.

4.4 Discussion

The primary contribution of this study was to evaluate if deep learning techniques could be applied to user state estimation for human augmentation robotics to produce even higher accuracy user state estimation models compared to the neural network-based models previously developed. Overall, the deep learning based models (CNN and LSTM) outperformed the neural network-based model with hand picked features (FCNN) in both gait phase estimation and walking speed estimation. The significant reduction of estimation error for the models represents the more robust learned intermediate representation of the feature set. This implies that the deep learning techniques can be applied to other areas of applied ma-

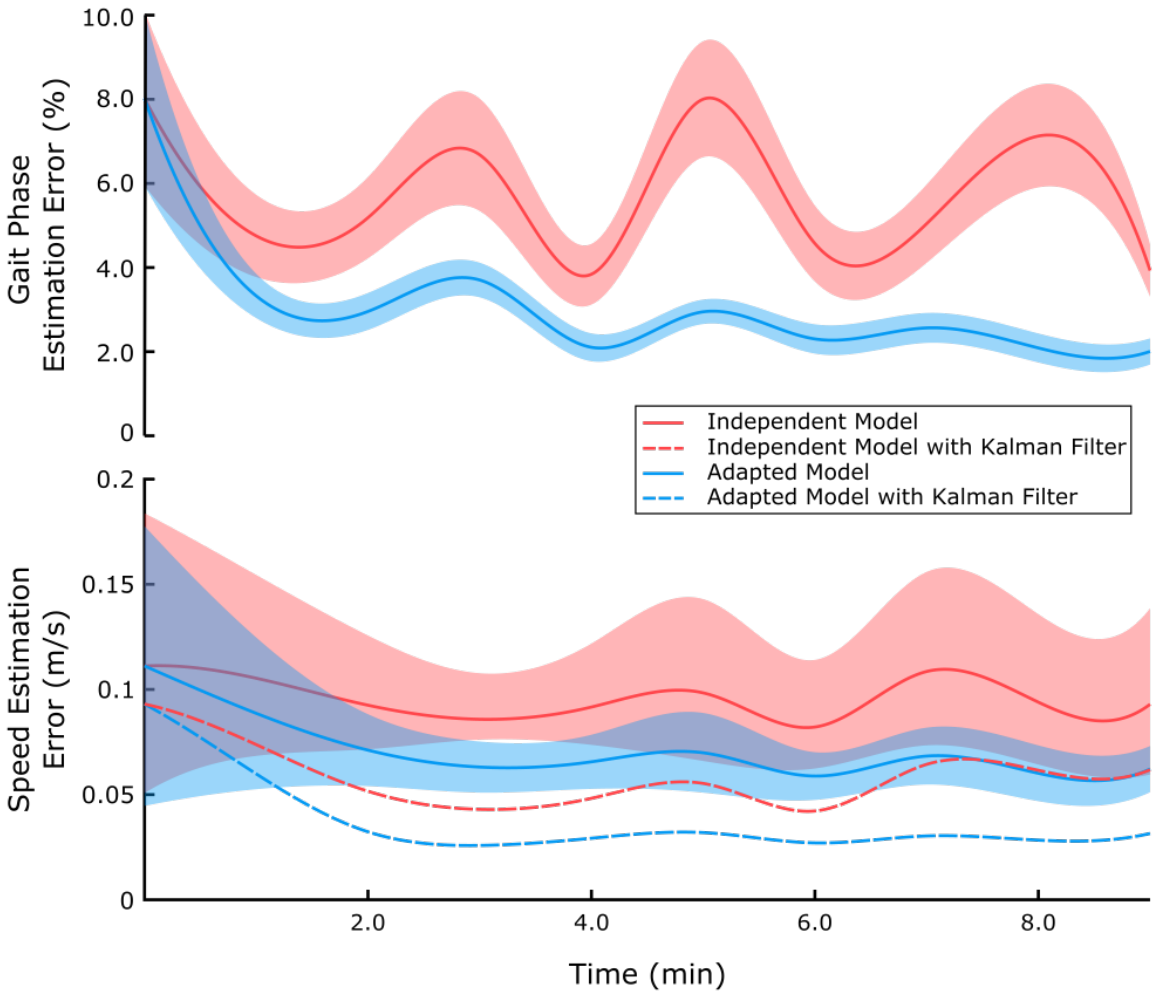

Figure 4.6: Simulation of adaptation performed offline. User-independent models for gait phase and walking speed estimation are simultaneously estimating and training on new data from an unseen testing user walking on a dynamic speed profile with accelerations and steady state. RMSE is averaged per 30 second intervals and shaded error bars are presented representing one standard deviation. Walking speed estimation is shown with and without the Kalman filter.

chine learning for human augmentation robotics such as locomotion mode classification, fall detection, or gait dynamics estimation.

The key difference in the deep learning-based models compared to the FCNN is the way in which the sliding window is used. Although all three models use the same sliding window approach to compute the features, the CNN and LSTM models operate on the data in a different way. The FCNN reduces the full window length of data for a single sensor into a single value via some mathematical operation such as mean, max, or standard deviation. Comparatively, the CNN uses a learned convolution filter to slide over the window and produce many different outputs depending on the convolution size. The LSTM operates even more differently, using a recurrent architecture to pass the data in the sliding window temporally and move the hidden state between temporal nodes. In the case of the CNN and LSTM, the temporal information is learned as a many-to-many paradigm rather than a many-to-one paradigm which is used in the FCNN, which adds to the feature diversity and makes the learning problem easier. Additionally, while the FCNN features are hand picked and invariant, both the LSTM and CNN can learn to change the way in which features are generated and the backpropagation through the network allows the models to learn a better intermediate representation.

This study demonstrated that machine learning-based estimators can accurately estimate the user state variable even when assistance is applied. Since previous studies have shown how hip exoskeleton assistance shifts gait biomechanics [7], the underlying process of learning user state variables could be affected by applying assistance. Both gait phase estimation and walking speed estimation was robust to the application of assistance, and demonstrated that user state variables can be estimated from machine learning-based models in a variety of scenarios. This is a key finding for the the exoskeleton community, since as various research groups test various controllers and their effect on mobility, the same user state estimation techniques can be applied instead of retraining them every time.

The simulation of adaptation implemented an idea of transfer learning called N-shot learning. In this style of learning, a model originally trained for a particular task is re-trained on a new task with new data. This allows the model to leverage previously learned ideas and representations and apply it to learning the new task. In this study, the models were originally trained as user-independent with no knowledge of the tested user. In the simulation of adaptation, the models were tasked with simultaneously estimating from the sensor values as well as training from the new data as it was seen by the model. This represents learning to a new task (user) for both gait phase and speed estimation. Overall the simulation showed that this process can significantly reduce estimation error for both gait phase and speed estimation. Additionally, the simulation demonstrated that the adaptation converges in roughly three minutes of walking. This implies that significantly less data is needed to adapt to a novel user compared to the amount of data a single user had in the user-independent training dataset.

One limitation of this study is that it was not an exhaustive search of all potential machine learning algorithms for gait phase and walking speed estimation. Although CNN and LSTM architectures were tested in this study, there may be other architectures that could perform much better for these user state estimation taks. Future work would include testing the adaptation of gait phase and walking speed estimation online in real-time for overground walking in the powered hip exoskeleton as well as testing novel machine learning models for user state estimation.

CHAPTER 5

PRELIMINARY RESULTS OF ONLINE ADAPTATION IN REAL-TIME

Given the success of developing deep learning-based user state estimation techniques for gait phase and walking speed estimation, a natural extension of the work is to implement the algorithms in real-time on the powered hip exoskeleton and evaluate the models in an overground walking task. Additionally, the promising results of the simulation of adaptation prompt an extension of the research to develop a real-time online adaptation system to learn while estimating on the hip exoskeleton. A study was performed to develop a real-time online adaptation system for the powered hip exoskeleton and test the system in overground walking. The hypothesis presented was that online adaptation of deep learning-based models will perform better than their user-independent counterparts. The goal of this study was to evaluate the performance of online real-time adaptation in the effort to maximize user state estimation performance but minimize the amount of user specific data needed to develop the machine learning-based methods.

5.1 Methods

5.1.1 Real-Time Online Adaptation System

Unlike previous studies which only used fully connected neural networks (FCNN) for user state estimation, deep learning models are much more mathematically complex, especially the convolutional neural networks (CNN) that performed the best for gait phase and speed estimation as previous studies had investigated. Although FCNN models could be

implemented natively on the hip exoskeleton due to their representation as a series of matrix multiplications, operations such as convolution or recurrency are much more difficult to implement natively on the hip exoskeleton control system. Because of this, a machine learning co-processor was needed. A Jetson Nano (NVIDIA, USA) was chosen as the co-processor to be used due to its small form factor, plethora of input and output options, as well as the 472 GFLOPs of compute power available. The Jetson Nano was connected to the hip exoskeleton via an ethernet cable, and TCP/IP was used to communicate between the devices. The hip exoskeleton sent the Jetson Nano the real-time sensor data at 100 Hz, as well as FSR voltage for gait phase labeling and the speed ground truth label. The Jetson Nano replied to the exoskeleton with the latest gait phase and walking speed estimates at 100 Hz.

The Jetson Nano has pre-built versions of Tensorflow which can take advantage of the built in GPU to accelerate real-time inference and training on the device. The Jetson Nano was programmed to have multiple concurrent threads in order to perform real-time inference, train on new data if needed, as well as interact with the operator via SSH (Fig. 5.1). The first thread was the data communication thread, which was set to be asynchronous. This thread handled the communication between the Jetson Nano and the hip exoskeleton and was clocked by the exoskeleton sending data. This thread also kept a data queue of 5 seconds across all signals which would be used for training data if needed. This thread latched the latest gait phase and speed estimations and replied to the hip exoskeleton to maintain 100 Hz of operating speed. The second thread was the real-time inference thread. In this thread, the most recent window of data was pulled from the data queue and passed through both the walking speed and gait phase estimation models. These estimations were sent back to the data handling thread to pass onto the exoskeleton. Additionally, if a flag for adaptation was set, weights for the latest trained model would be pulled from a file when the gait phase estimation model detected a heel contact ($g = 0$). Finally, the last thread was the real-time training thread. This thread was responsible for labeling the data from the

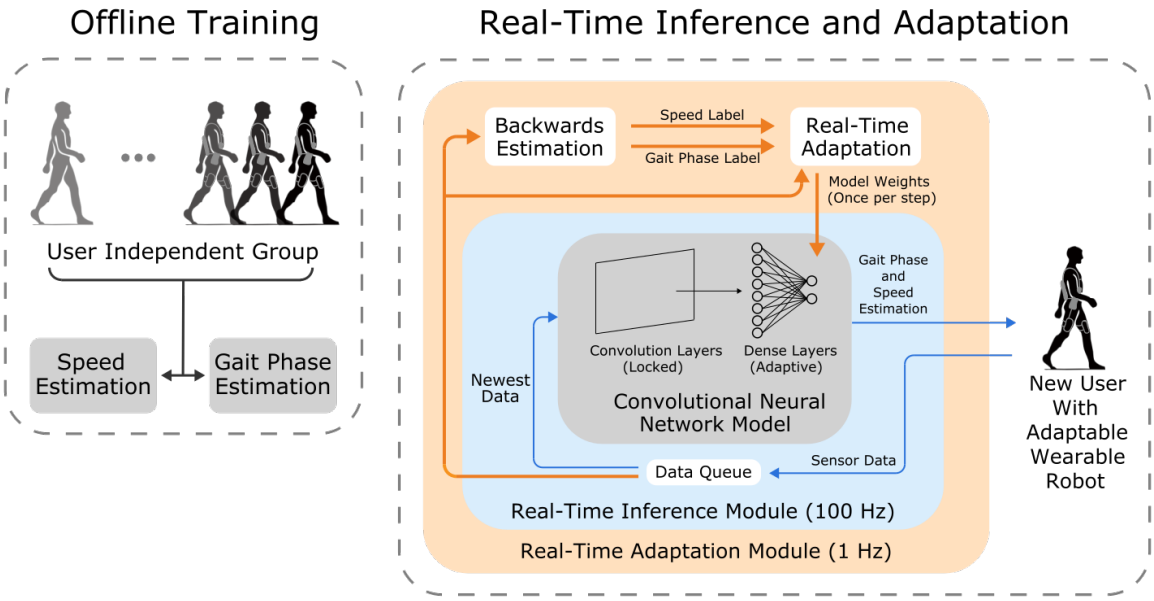

Figure 5.1: Illustration of concurrent processes for real-time online adaptation with the hip exoskeleton. Offline, models for gait phase and speed estimation are developed from a user-independent pool of subjects. In real-time, with a novel subject, data is transmitted from the exoskeleton to the machine learning co-processor and passed through the models for real-time inference at 100 Hz. Additionally, this data is queued and labeled at 1Hz to then be used for adaptation, updating the inference models at heel contact.

exoskeleton, generating a training set, training the models, and saving the model weights to a file. At every heel contact (determined by the FSR voltage), the gait phase from the previous heel contact could be labeled as linearly increasing from 0% to 100%. The speed label was passed from the treadmill control desk to the exoskeleton via a PWM signal, and was thus sent to the Jetson Nano as a numeric label and no modifications were necessary. This training thread generated a data set from the full 5 seconds of data in the data queue and then trained each model on the data seen. The weights were saved to a file so they could be loaded by the real-time inference thread later. The models for real-time training had the convolutional layers locked to optimize speed of training.

5.1.2 Experimental Protocol

The study was approved by the Georgia Institute of Technology Institutional Review Board, and informed written consent was obtained for all subjects. The study was approved by the Georgia Institute of Technology Institutional Review Board, and informed written consent was obtained for all subjects. A single subject walked on a treadmill wearing the hip exoskeleton device while the treadmill speed was set according to a predefined trajectory (Fig. 5.2). Mechanical sensor data was recorded such as the hip encoder angle, the right thigh IMU acceleration and gyroscope measurements, the trunk IMU acceleration and gyroscope measurements, as well as machine learning estimations for gait phase and walking speed. The FSR voltage was collected on the device so that the ground truth gait phase percentage could be computed retroactively. The ground truth speed was sent from the treadmill controller to the exoskeleton via a 10-bit PWM signal and recorded on device at 100 Hz. During the trial, the deep learning models for gait phase and speed estimation were set to adapt based on the new data while estimating in real-time. The estimates for gait phase and walking speed were used in Equation 5.1 in order to apply assistance to the user, where g represents gait phase percentage for a single leg, s represents the walking speed, and $\mathcal{N}(\mu, \sigma^2)$ represents the Gaussian probability density function with mean μ and variance σ^2.

$$\tau(g, s) = 10s\mathcal{N}(g - 5, 64) - 7s\mathcal{N}(g - 55, 64) + 10s\mathcal{N}(g - 105, 64) \tag{5.1}$$

Additionally, the single subject walked wearing the hip exoskeleton device overground while the user-independent machine learning estimators were used in real-time. Assistance was applied via Equation 5.1, and the ground truth speed was measured with a Vicon motion capture system. The estimations were recorded on the device, as well as the FSR voltage for ground truth labeling only. The subject walked back and forth overground 8

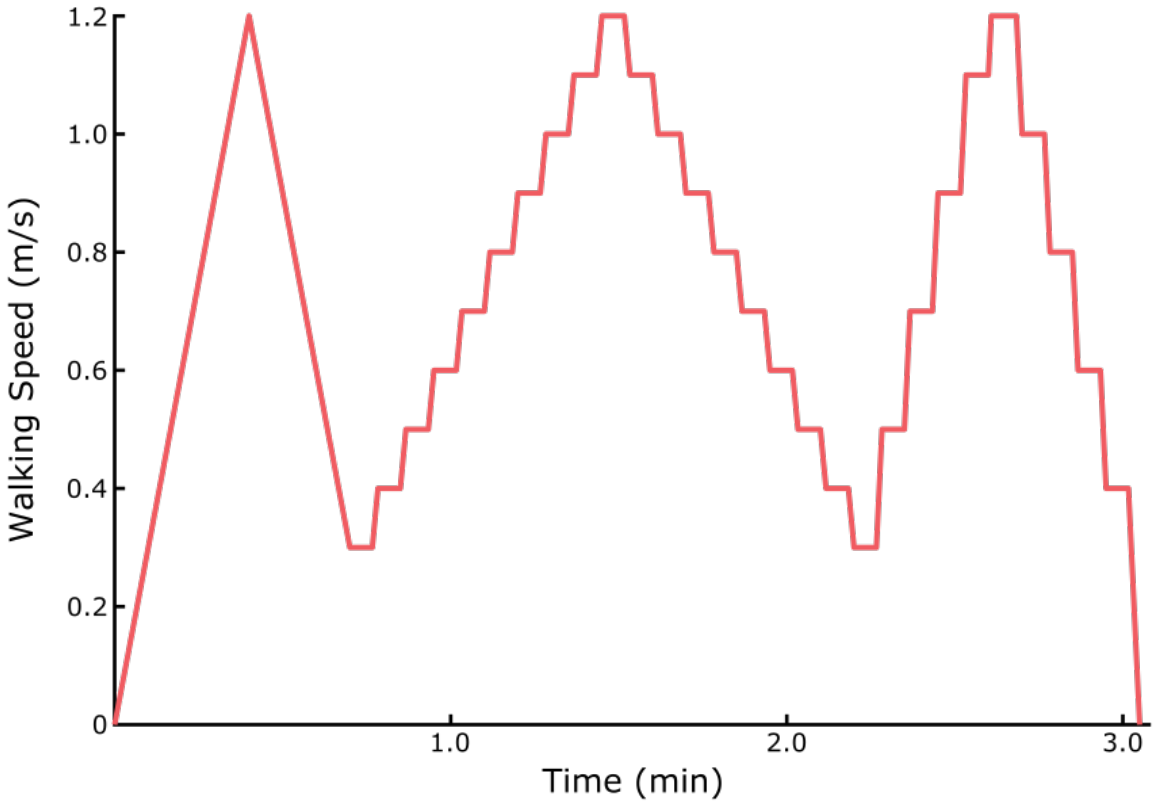

Figure 5.2: Speed profile used for the adaptation trial condition. Treadmill speed is set according to a velocity trajectory, moving between speeds of 0.3 m/s to 1.2 m/s. Three different sections contain different acceleration settings, and steady state walking is also captured.

total times, and the data was recorded to evaluate the performance of the machine learning estimator in the overground scenarios.

5.2 Results

Overall, the online adaptation system was able to estimate and train from the data in real-time. On average, inference took 0.006 s per iteration and training took 0.482 s per iteration. In terms of gait phase estimation performance, the initial error of the deep learning model was 11.30 %, but by the end of the trial the gait phase estimation error was 2.77%. This represents a 75.5% reduction in gait phase estimation error by the online adaptation system. For speed estimation, the initial speed estimation error of the deep learning model was 0.215 m/s but by the end of the trial, the speed estimation error was 0.03 m/s. This represents a 86% reduction in error by the online adapted system.

For the overground walking section, both gait phase and speed estimation performed well. Gait phase estimation tracked well during the walking motions (Fig. 5.3, but failed to adequately capture stopped motion during the turns in the overground scenario. The overall RMSE of the gait phase estimation using the user-independent model was 14.19%. Speed estimation also tracked well during walking motions (Fig. 5.4), but the speed estimations failed to reach 0 m/s during stopping motions, and only fell to about 0.2 m/s minimum. Overall, the RMSE of the speed estimation using the user-independent model was 0.22 m/s.

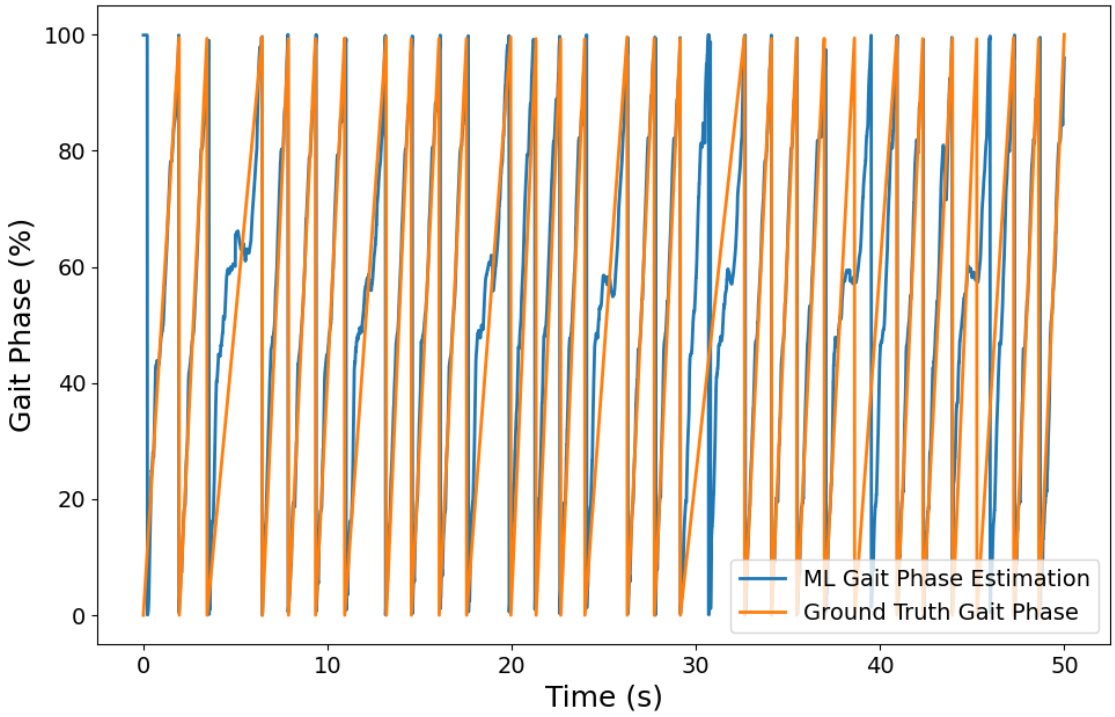

Figure 5.3: Gait phase estimation during the overground walking trial. The machine learning estimation from the user-independent model is shown against the ground truth which was computed retroactively from the FSR voltage.

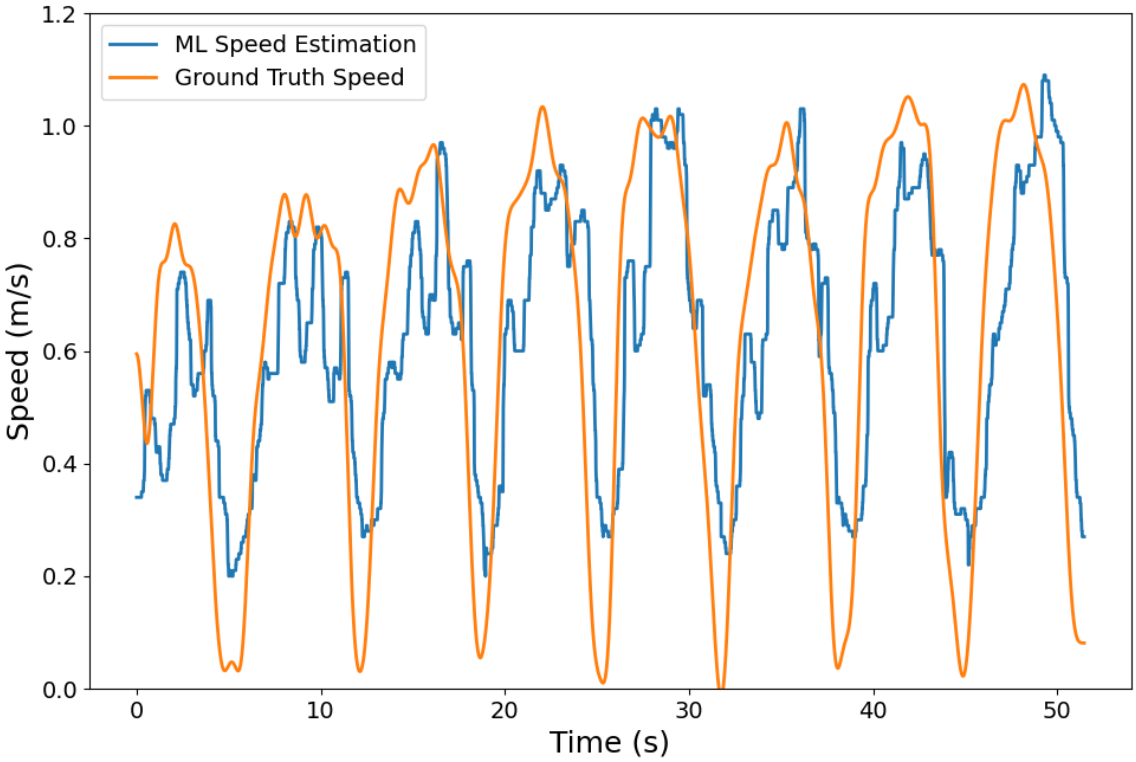

Figure 5.4: Speed estimation during the overground walking trial. The machine learning estimation from the user-independent model is shown against the ground truth which was computed retroactively from the Vicon motion capture system.

CHAPTER 6

DISCUSSION

User state estimation is an important factor for high-level control of exoskeleton devices. Although common user state estimation tasks exist, they are limited to very specific scenarios or fair to work in the various tasks in which exoskeletons are poised to assist users. Although machine learning is used elsewhere in the field, they are often limited to classification tasks or intent recognition. The work presented in this thesis is the first implementation of regression of user state estimation using machine learning tasks for powered hip exoskeletons. Furthermore, the machine learning-based estimation techniques performed better than traditional methods in restricted scenarios such as treadmill walking at steady speed, as well as new dynamic scenarios such as dynamic speed walking or overground walking. Various methods to best estimate user state variables such as gait phase, walking speed, and inclination angle were explored. The various sensors that contribute to these estimation tasks, as well as the optimal machine learning models were investigated. Overall, the results yielded low error user state estimation techniques that can be implemented in real-time for the hip exoskeleton to modulate assistance in dynamic walking scenarios, vastly improving the ability of exoskeleton technology beyond simple treadmill walking.

For all machine learning tasks, data is at the heart of the learning paradigm: without an expansive and thorough dataset, learning the fundamental task can be difficult. This is the case when dealing with machine learning models for human augmentation robotics, as it is expensive to collect data using human subjects. One key method to combat this issue is to leverage many subjects and compile them together in a single dataset. How-

ever, this user-independent strategy fails to collect adequate data for a single subject and is left with non-negligible steady state error for all estimation tasks. The work in this thesis presents a solution to this issue: online adaptation. By starting with a pre-trained user-independent model, and then additionally training on new data, the amount of subject specific data greatly decreases compared to if a user-dependent model was to be created originally. This is due to the fact that the online adaptation can leverage what was learned from the user-independent dataset and then adapt to the specific user's gait dynamics for the state estimation tasks. Additionally, this adaptation happens very quickly: the preliminary results indicate less than 3 minutes of new data is required to reduce error rates of gait phase and walking speed estimation significantly (50% or more).

Although the research presented here does not encapsulate the most optimal user state estimation techniques, various methods of using ideas from machine learning are presented and applied to the hip exoskeleton field. One big limitation from this research is the lack of a very large data set with a large number of subjects. Machine learning tasks benefit from training on adverse data, but to do this a large amount of data is needed, much more than what is presented in this thesis. Furthermore, the CNN and LSTM models tested and used in the final studies were at the time of development state-of-the-art but given the pace of machine learning research will naturally be outclassed in time. It is likely a newer machine learning technology will be able to learn the dynamics of hip exoskeleton data better and result in higher accuracy user state estimation in even more dynamic scenarios such as community ambulation.

The work presented in this thesis represents development of high-level user state estimation techniques. This information is crucial for exoskeleton developers and researchers so they can use this information in their control strategies. One such control strategy is presented in this thesis: where assistance magnitude scales with walking speed and is affected by gait phase as a timing variable. Although this strategy is not purported to be optimal

by any standards, it demonstrates how user state estimation can directly influence assistance profiles. Since these assistance profiles are at the forefront of research to minimize energetic expenditure of walking as much as possible, the methods presented in this thesis represent a large step towards creating a new class of assistance profiles that will allow the exoskeleton community to investigate even more control paradigms.

CHAPTER 7

CONCLUSION AND FUTURE WORK

This thesis investigated how machine learning techniques can be used to estimate user state in a powered hip exoskeleton. First, an investigation was performed to see how neural networks could be used to learn gait phase estimation in real-time on the hip exoskeleton. The hypothesis presented was that neural network-based gait phase estimation would perform better than time-based estimation on treadmill walking at various speeds. The results indicated that at worst, the machine learning models performed the same as the time-based estimation strategy and during dynamic speed motion, the machine learning-based estimators performed significantly better. Next, an investigation was performed to evaluate how biological sensors such as EMG could be used to improve walking speed or inclination angle estimation. The second hypothesis presented is that using biological sensor information with machine learning-based estimators for walking speed and inclination angle will reduce estimation error compared to machine learning-based estimators using only mechanical sensor data on the hip exoskeleton. The results showed that this was the case for able-bodied subjects, where the addition of EMG sensors reduced the estimation error for incline and speed estimation, but the results from the elderly pool did not indicate this. The final hypothesis presented is that online adaptation of deep learning-based models for gait phase and walking speed estimation will reduce estimation error compared to user-independent deep learning-based models for overground walking of able-bodied subjects wearing the powered hip exoskeleton. Preliminary results show that online adaptation is successful in reducing error of walking speed and gait phase estimation by more than 50%. Future work includes evaluating online adaptation of gait phase and walking speed esti-

mation overground, in dynamic incline scenarios, and in community ambulation. Further machine learning ideas can be investigated in their capacity to improve control strategies for hip exoskeletons such as N-shot learning, imitation learning, and reinforcement learning.

REFERENCES

[1] A. J. Young and D. P. Ferris, "State of the art and future directions for lower limb robotic exoskeletons," *IEEE Transactions on Neural Systems and Rehabilitation Engineering*, vol. 25, no. 2, pp. 171–182, Feb. 2017.

[2] G. S. Sawicki, O. N. Beck, I. Kang, and A. J. Young, "The exoskeleton expansion: Improving walking and running economy," *Journal of NeuroEngineering and Rehabilitation*, vol. 17, no. 1, p. 25, Feb. 19, 2020.

[3] G. S. Sawicki, C. L. Lewis, and D. P. Ferris, "It pays to have a spring in your step:" *Exercise and Sport Sciences Reviews*, vol. 37, no. 3, pp. 130–138, Jul. 2009.

[4] Y. Kusuda, "In quest of mobility – honda to develop walking assist devices," *Industrial Robot: An International Journal*, vol. 36, no. 6, pp. 537–539, Jan. 1, 2009, Publisher: Emerald Group Publishing Limited.

[5] K. Seo, J. Lee, Y. Lee, T. Ha, and Y. Shim, "Fully autonomous hip exoskeleton saves metabolic cost of walking," in *2016 IEEE International Conference on Robotics and Automation (ICRA)*, May 2016, pp. 4628–4635.

[6] Y. Ding, M. Kim, S. Kuindersma, and C. J. Walsh, "Human-in-the-loop optimization of hip assistance with a soft exosuit during walking," *Science Robotics*, vol. 3, no. 15, Feb. 28, 2018, Publisher: Science Robotics Section: Research Article.

[7] I. Kang, H. Hsu, and A. Young, "The effect of hip assistance levels on human energetic cost using robotic hip exoskeletons," *IEEE Robotics and Automation Letters*, vol. 4, no. 2, pp. 430–437, Apr. 2019.

[8] A. Alamdari and V. N. Krovi, "Chapter two - a review of computational musculoskeletal analysis of human lower extremities," in *Human Modelling for Bio-Inspired Robotics*, J. Ueda and Y. Kurita, Eds., Academic Press, Jan. 1, 2017, pp. 37–73, ISBN: 978-0-12-803137-7.

[9] A. J. Young, J. Foss, H. Gannon, and D. P. Ferris, "Influence of power delivery timing on the energetics and biomechanics of humans wearing a hip exoskeleton," *Frontiers in Bioengineering and Biotechnology*, vol. 5, Mar. 8, 2017.

[10] C. L. Lewis and D. P. Ferris, "Invariant hip moment pattern while walking with a robotic hip exoskeleton," *Journal of biomechanics*, vol. 44, no. 5, pp. 789–793, Mar. 15, 2011.

[11] P. Malcolm, W. Derave, S. Galle, and D. D. Clercq, "A simple exoskeleton that assists plantarflexion can reduce the metabolic cost of human walking," *PLOS ONE*, vol. 8, no. 2, e56137, Feb. 13, 2013, Publisher: Public Library of Science.

[12] D. Quintero, D. J. Lambert, D. J. Villarreal, and R. D. Gregg, "Real-time continuous gait phase and speed estimation from a single sensor," in *2017 IEEE Conference on Control Technology and Applications (CCTA)*, Aug. 2017, pp. 847–852.

[13] D. J. Villarreal, D. Quintero, and R. D. Gregg, "Piecewise and unified phase variables in the control of a powered prosthetic leg," in *2017 International Conference on Rehabilitation Robotics (ICORR)*, ISSN: 1945-7901, Jul. 2017, pp. 1425–1430.

[14] R. Ronsse, T. Lenzi, N. Vitiello, B. Koopman, E. van Asseldonk, S. M. M. De Rossi, J. van den Kieboom, H. van der Kooij, M. C. Carrozza, and A. J. Ijspeert, "Oscillator-based assistance of cyclical movements: Model-based and model-free approaches," *Medical & Biological Engineering & Computing*, vol. 49, no. 10, p. 1173, Sep. 1, 2011.

[15] F. Giovacchini, F. Vannetti, M. Fantozzi, M. Cempini, M. Cortese, A. Parri, T. Yan, D. Lefeber, and N. Vitiello, "A light-weight active orthosis for hip movement assistance," *Robotics and Autonomous Systems*, Wearable Robotics, vol. 73, pp. 123–134, Nov. 1, 2015.

[16] J. J. Eng and D. A. Winter, "Kinetic analysis of the lower limbs during walking: What information can be gained from a three-dimensional model?" *Journal of Biomechanics*, vol. 28, no. 6, pp. 753–758, Jun. 1995.

[17] Q. Li, M. Young, V. Naing, and J. M. Donelan, "Walking speed and slope estimation using shank-mounted inertial measurement units," in *2009 IEEE International Conference on Rehabilitation Robotics*, Jun. 2009, pp. 839–844.

[18] ——, "Walking speed estimation using a shank-mounted inertial measurement unit," *Journal of Biomechanics*, vol. 43, no. 8, pp. 1640–1643, May 28, 2010.

[19] K. Seo, Y. J. Park, J. Lee, S. Hyung, M. Lee, J. Kim, H. Choi, and Y. Shim, "RNN-based on-line continuous gait phase estimation from shank-mounted IMUs to control ankle exoskeletons," in *2019 IEEE 16th International Conference on Rehabilitation Robotics (ICORR)*, ISSN: 1945-7901, Jun. 2019, pp. 809–815.

[20] A. J. Young, T. A. Kuiken, and L. J. Hargrove, "Analysis of using EMG and mechanical sensors to enhance intent recognition in powered lower limb prostheses," *Journal of Neural Engineering*, vol. 11, no. 5, p. 056 021, Oct. 2014.

[21] Y. LeCun, Y. Bengio, and G. Hinton, "Deep learning," *Nature*, vol. 521, no. 7553, pp. 436–444, May 2015, Number: 7553 Publisher: Nature Publishing Group.

[22] J. Schmidhuber, "Deep learning in neural networks: An overview," *Neural Networks*, vol. 61, pp. 85–117, Jan. 2015. arXiv: 1404.7828.

[23] H. T. T. Vu, F. Gomez, P. Cherelle, D. Lefeber, A. Nowé, and B. Vanderborght, "ED-FNN: A new deep learning algorithm to detect percentage of the gait cycle for powered prostheses," *Sensors*, vol. 18, no. 7, p. 2389, Jul. 2018.

[24] I. Goodfellow, Y. Bengio, and A. Courville, *Deep Learning*. MIT Press, 2016, http://www.deeplearningbook.org.

[25] A. J. Young and L. J. Hargrove, "A classification method for user-independent intent recognition for transfemoral amputees using powered lower limb prostheses," *IEEE Transactions on Neural Systems and Rehabilitation Engineering*, vol. 24, no. 2, pp. 217–225, Feb. 2016, Conference Name: IEEE Transactions on Neural Systems and Rehabilitation Engineering.

[26] J. A. Spanias, A. M. Simon, S. B. Finucane, E. J. Perreault, and L. J. Hargrove, "Online adaptive neural control of a robotic lower limb prosthesis," *Journal of Neural Engineering*, vol. 15, no. 1, p. 016 015, 2018.

[27] M. Liu, F. Zhang, and H. H. Huang, "An adaptive classification strategy for reliable locomotion mode recognition," *Sensors (Basel, Switzerland)*, vol. 17, no. 9, Sep. 4, 2017.

[28] I. Kang, H. Hsu, and A. J. Young, "Design and validation of a torque controllable hip exoskeleton for walking assistance," presented at the ASME 2018 Dynamic Systems and Control Conference, American Society of Mechanical Engineers Digital Collection, Nov. 12, 2018.

[29] I. Kang, P. Kunapuli, H. Hsu, and A. J. Young, "Electromyography (EMG) signal contributions in speed and slope estimation using robotic exoskeletons," in *2019 IEEE 16th International Conference on Rehabilitation Robotics (ICORR)*, ISSN: 1945-7901, 1945-7898, Jun. 2019, pp. 548–553.

[30] I. Kang, P. Kunapuli, and A. J. Young, "Real-time neural network-based gait phase estimation using a robotic hip exoskeleton," *IEEE Transactions on Medical Robotics and Bionics*, vol. 2, no. 1, pp. 28–37, Feb. 2020, Conference Name: IEEE Transactions on Medical Robotics and Bionics.

[31] H. A. Varol, F. Sup, and M. Goldfarb*, "Multiclass real-time intent recognition of a powered lower limb prosthesis," *IEEE Transactions on Biomedical Engineering*, vol. 57, no. 3, pp. 542–551, Mar. 2010, Conference Name: IEEE Transactions on Biomedical Engineering.

[32] R. Bellman, *Dynamic Programming*, 1st ed. Princeton, NJ, USA: Princeton University Press, 1957.

[33] F. Chollet *et al.*, *Keras*, `https://keras.io`, 2015.

[34] M. Abadi, A. Agarwal, P. Barham, E. Brevdo, Z. Chen, C. Citro, G. S. Corrado, A. Davis, J. Dean, M. Devin, S. Ghemawat, I. Goodfellow, A. Harp, G. Irving, M. Isard, Y. Jia, R. Jozefowicz, L. Kaiser, M. Kudlur, J. Levenberg, D. Mané, R. Monga, S. Moore, D. Murray, C. Olah, M. Schuster, J. Shlens, B. Steiner, I. Sutskever, K. Talwar, P. Tucker, V. Vanhoucke, V. Vasudevan, F. Viégas, O. Vinyals, P. Warden, M. Wattenberg, M. Wicke, Y. Yu, and X. Zheng, *TensorFlow: Large-scale machine learning on heterogeneous systems*, Software available from tensorflow.org, 2015.

[35] V. K. Ojha, A. Abraham, and V. Snášel, "Metaheuristic design of feedforward neural networks: A review of two decades of research," May 16, 2017.

[36] D. P. Kingma and J. Ba, "Adam: A method for stochastic optimization," *arXiv:1412.6980 [cs]*, Dec. 22, 2014. arXiv: `1412.6980`.

[37] I. Sutskever, J. Martens, and G. Dahl, "On the importance of initialization and momentum in deep learning," p. 9, Jun. 16, 2013.

[38] Y. Ding, I. Galiana, C. Siviy, F. A. Panizzolo, and C. Walsh, "IMU-based iterative control for hip extension assistance with a soft exosuit," in *2016 IEEE International Conference on Robotics and Automation (ICRA)*, May 2016, pp. 3501–3508.

[39] T. G. Sugar, A. Bates, M. Holgate, J. Kerestes, M. Mignolet, P. New, R. K. Ramachandran, S. Redkar, and C. Wheeler, "Limit cycles to enhance human performance based on phase oscillators," *Journal of Mechanisms and Robotics*, vol. 7, no. 1, Feb. 1, 2015, Publisher: American Society of Mechanical Engineers Digital Collection.

[40] T. Yan, A. Parri, V. Ruiz Garate, M. Cempini, R. Ronsse, and N. Vitiello, "An oscillator-based smooth real-time estimate of gait phase for wearable robotics," *Autonomous Robots*, vol. 41, no. 3, pp. 759–774, Mar. 1, 2017.

[41] K. Seo, S. Hyung, B. K. Choi, Y. Lee, and Y. Shim, "A new adaptive frequency oscillator for gait assistance," in *2015 IEEE International Conference on Robotics and Automation (ICRA)*, ISSN: 1050-4729, May 2015, pp. 5565–5571.

[42] S. J. Pan and Q. Yang, "A survey on transfer learning," *IEEE Transactions on Knowledge and Data Engineering*, vol. 22, no. 10, pp. 1345–1359, Oct. 2010.

[43] H. Huang, T. A. Kuiken, and R. D. Lipschutz, "A strategy for identifying locomotion modes using surface electromyography," *IEEE Transactions on Biomedical Engi-*

neering, vol. 56, no. 1, pp. 65–73, Jan. 2009, Conference Name: IEEE Transactions on Biomedical Engineering.

[44] A. J. Young, A. M. Simon, and L. J. Hargrove, "A training method for locomotion mode prediction using powered lower limb prostheses," *IEEE Transactions on Neural Systems and Rehabilitation Engineering*, vol. 22, no. 3, pp. 671–677, May 2014, Conference Name: IEEE Transactions on Neural Systems and Rehabilitation Engineering.

[45] H. Huang, F. Zhang, L. J. Hargrove, Z. Dou, D. R. Rogers, and K. B. Englehart, "Continuous locomotion-mode identification for prosthetic legs based on neuromuscular-mechanical fusion," *IEEE transactions on bio-medical engineering*, vol. 58, no. 10, pp. 2867–2875, Oct. 2011.

[46] Y. LeCun, P. Haffner, L. Bottou, and Y. Bengio, "Object recognition with gradient-based learning," in *Shape, Contour and Grouping in Computer Vision*, ser. Lecture Notes in Computer Science, D. A. Forsyth, J. L. Mundy, V. di Gesú, and R. Cipolla, Eds., Berlin, Heidelberg: Springer, 1999, pp. 319–345, ISBN: 978-3-540-46805-9.

[47] S. Hochreiter and J. Schmidhuber, "Long short-term memory," *Neural Computation*, vol. 9, no. 8, pp. 1735–1780, Nov. 1, 1997.

[48] U. Côté Allard, F. Nougarou, C. L. Fall, P. Giguère, C. Gosselin, F. Laviolette, and B. Gosselin, "A convolutional neural network for robotic arm guidance using sEMG based frequency-features," in *2016 IEEE/RSJ International Conference on Intelligent Robots and Systems (IROS)*, ISSN: 2153-0866, Oct. 2016, pp. 2464–2470.